



VYSOKÉ UČENÍ TECHNICKÉ V BRNĚ
BRNO UNIVERSITY OF TECHNOLOGY



FAKULTA CHEMICKÁ
ÚSTAV CHEMIE MATERIÁLŮ

FACULTY OF CHEMISTRY
INSTITUTE OF MATERIALS SCIENCE

STRUCTURE AND PROPERTIES OF COLLAGEN/HAP NANOCOMPOSITE NETWORKS

STRUKTURA A VLASTNOSTI NANOKOMPOZITNÍCH SÍTÍ KOLAGEN/HAP

DOKTORSKÁ PRÁCE
DOCTORAL THESIS

AUTOR PRÁCE
AUTHOR

Mgr. EMA JANČÁŘOVÁ

VEDOUCÍ PRÁCE
SUPERVISOR

prof. RNDr. JOSEF JANČÁŘ, CSc.

BRNO 2014

ABSTRACT

This thesis is focused on the kinetics of self-assembly and mechanical properties of collagen solutions. The effect of hydroxyapatite nanoparticles on the collagen self-assembly and mechanical properties is also investigated. Possible mechanisms of collagen/hydroxyapatite interactions are elucidated along with the description of structure evolution and properties at various structural levels. The shear rate dependences and viscoelastic behavior of collagen and its nanocomposites with hydroxyapatite (HAP) were measured and interpreted molecularly. Finally, the results were discussed in terms of the applicability of collagen/hydroxyapatite nanocomposites in scaffolds for bone tissue regeneration.

SHRNUTÍ

Tato práce je zaměřena na samouspořádací procesy, kinetiku, obecné zákonitosti řídící proces samouspořádání a mechanické vlastnosti kolagenních roztoků. Dále je zkoumán efekt hydroxyapatitových nanočástic na samouspořádání kolagenu a mechanické vlastnosti výsledných nanokompozitních hydrogelů. Jsou objasněny možné mechanismy interakcí mezi kolagenem I a hydroxyapatitem spolu s popisem vývoje struktury a vlastností na různých úrovních struktury. Byly měřeny a molekulárně interpretovány závislosti viskoelastických veličin na smykové rychlosti spolu s viskoelastickým chováním. Závěrem byly diskutovány výsledky v souvislosti s jejich aplikovatelností v tkáňovém inženýrství chrupavek tvrdých tkání a v regenerativní medicíně.

KEY WORDS

Collagen self-assembly, mechanical properties of protein materials, tissue engineering, bone, fibrillogenesis, rheology, hydroxyapatite, nanocomposites

KLÍČOVÁ SLOVA

Samouspořádávání kolagenu, mechanické vlastnosti proteinových materiálů, tkáňové inženýrství, kosti, fibrilogeneze, reologie, hydroxyapatit, nanokompozity

TABLE OF CONTENTS

ABSTRACT	2
SHRNUTÍ	2
KEY WORDS.....	2
KLÍČOVÁ SLOVA	3
1 INTRODUCTION	4
2 REVIEW OF LITERATURE.....	6
2.1 Tissue engineering	6
2.2 Collagen	7
2.3 Collagen self-assembly, fibrillogenesis	7
2.4 Biomineralization.....	9
2.5 Collagen/HAP nanocomposites	9
2.6 Hierarchical collagen-based tissues: bone	10
2.7 Hydrogel viscoelasticity.....	11
3 GOALS OF THE THESIS	11
4 RESULTS, DISCUSSION	12
4.1 Determining the linear viscoelastic interval.....	12
4.2 Reinforcing mechanisms in coll/HAP nanocomposite gels	18
4.3 Kinetics of gelation	25
4.4 The dependence of viscosity on the shear rate.....	34
4.5 Morphology of freeze-dried collagen	37
4.6 Use of freeze-dried collagen/HAP networks in bone tissue engineering.....	39
5 CONCLUSION	41
6 REFERENCES	43
7 CURRICULUM VITAE	47

1 INTRODUCTION

Damaged or diseased skeletal tissue frequently leads to progressive debilitation resulting in a marked decrease in the quality of life. Current approaches in bone engineering are mainly focused on the restoration of pathologically altered tissue structure based on the transplantation of mesenchymal stem cells in combination with supportive scaffolds. Although ceramics and metallic materials have been widely accepted for the development of implants, their non-resorbability and necessity of second surgical operation limit their applications in tissue engineering.

Tailored biomaterials with tunable functional properties have become increasingly important in medical applications due to their desired balance of properties and excellent host response in the field of regenerative medicine, tissue engineering and controlled drug delivery. To improve the predictability of biopolymer materials functionality, multiple design parameters need to be considered, along with appropriate models.

Self-organization is a fundamental process in which many biological structures are assembled from cell produced building blocks. (1) (2) The focus of this Thesis is to contribute to the fundamental understanding of hierarchical self-assembly of collagen I, the most frequent structural protein in mammals.

Collagen is the primary structural material in vertebrate biology, determining the mechanical behavior of musculoskeletal and connective tissues such as tendon, bone, tooth and skin. Collagen constitutes one-third of the human proteome, providing mechanical stability, elasticity, and strength to hard and soft tissues. Collagen is also the dominating material in the extracellular matrix and its stiffness controls cell differentiation, growth and pathology.

Despite extensive efforts in the investigation of the origin of collagen's unique mechanical properties, a full understanding of the relationship between its

molecular structure and mechanical properties remains elusive, hindered by the complex hierarchical structure of collagen-based tissues. In particular, although extensive studies of viscoelastic properties have been pursued at the macroscopic (fiber/tissue) level, fewer investigations have been performed at the smaller scales, including, in particular, collagen molecules and fibrils. These scales are, however, important for a complete understanding of the role of collagen as an important constituent in the extracellular matrix. (3)

Although the mechanical properties of collagen itself have been broadly studied experimentally, its self-assembly in the presence of hydroxyapatite nanoparticles (nHAP) has not been investigated to date. The effect of nHAP on collagen self-assembly in solution and on the mechanical properties of coll/nHAP nanocomposite solutions/hydrogels has to be determined in order to enable new bone tissue engineering strategies to be developed.

Most of the existing mechanical models describing the effects of local nano-structure on the mechanical response of bone consider regular distribution of simple shaped rigid inclusions in a polymer continuum. Despite the fact that the discrete nature of the structure at the nano-scale is acknowledged in these models, the fundamental effects related to the molecular nature of the proteins forming the matrix are neglected and the fact that due to the highly non-local response of polymers, the classical continuum mechanics is of limited validity is not taken into consideration. It has been suggested that the validity of continuum elasticity models can be extended to account for the nano-scale non-locality of deformation response of polymeric component by using higher order elasticity combined with molecular dynamics.

2 REVIEW OF LITERATURE

Most natural (or biological) materials are complex composites whose mechanical properties are often outstanding, considering the weak constituents from which they are assembled. Their defining characteristics are hierarchy, multifunctionality and a self-healing capability. Self-organization is also a fundamental feature of many biological materials and the manner by which the structures are assembled from the molecular level up. Biological materials can be divided into polypeptides (proteins), polysaccharides and nucleic acids depending upon the building blocks they are composed of. (1) In the presented work, we focus on proteins, specifically collagen I.

With the recent development of experimental techniques, the research of biomaterials has expanded into the micro- and nano-scale which has allowed the design of novel advanced synthetic functional materials. (8)

2.1 TISSUE ENGINEERING

Biomaterials play a very important role in tissue engineering. Numerous scaffolds produced from a variety of biomaterials have been used in the biomedical field in attempts to regenerate different tissues and organs in the body. (9) Collagen, being the main protein of connective tissue and skin, as an extracellular matrix protein, is widely used as a biomaterial for tissue regeneration and implantation. (10) (11) Practically all tissues are capable of being repaired by tissue engineering principles, which usually include a scaffold conducive to cell attachment and maintenance of cell function. Recent advances in the fields of biomaterials, biomateriomics, and tissue engineering have focused attention on the potentials for clinical application. (12) (13) (14) (15) (16)

The goal of tissue engineering is to produce a scaffold material that will guide cells to differentiate and regenerate functional replacement tissue at the site of

injury. (17) The extracellular matrix (ECM) is by definition nature's ideal biological scaffold material and its mechanical properties are largely a consequence of its collagen fiber architecture and kinematics. (18)

The last years have seen continuous refinement and improvement of tissue engineering strategies, but a number of tough practical problems persists. (15) (19) These are connected to the complex and truly multidisciplinary nature of this field, which integrates knowledge from polymer material properties, micro- and macro-structure of scaffolds, biomechanics, cell biology, etc. (20) (21) The tissue engineering field of interest in our case is bone TE.

2.2 COLLAGEN

Collagen represents the most abundant structural protein in mammals, providing mechanical stability, elasticity, and strength to connective tissues such as tendons, ligaments, and bone, as well as the extracellular matrix (ECM). It is known that virtually all collagen-based tissues are organized into hierarchical structures, where the lowest hierarchical level consists of triple helical collagen molecules. (6)

Collagen consists of tropocollagen (TC) molecules that have a length $L \approx 280nm$ and diameter of $\approx 1,5nm$. Staggered arrays of TC molecules form microfibrils, which arrange to form collagen fibers. (22) It has been long known that the stability of the collagen triple helix is related to the total content of amino acids proline and hydroxyproline, which together make up about 20% of the total (23)amino acids in human fibrous collagens. (23) (24)

2.3 COLLAGEN SELF-ASSEMBLY, FIBRILLOGENESIS

Self-assembly in the classic sense can be defined as the spontaneous and reversible organization of molecular units into ordered structures by non-covalent interactions. (25) The first property of a self-assembled system this definition suggests is the spontaneity of the self-assembly process: the interactions

responsible for the formation of the self-assembled system act on a strictly local level – in other words, the nanostructure builds itself.

Collagen fibrils are formed by the self-assembly of individual collagen molecules in a process referred to as fibrillogenesis. It has been established that the formation of collagen fibrils is a spontaneous process initiated by the enzymatic cleavage of procollagen propeptides. (26) (27) (28) The fibrils vary in length and diameter depending on the conditions involved in growth. However, typically in vitro formed fibrils are up to 500nm in diameter, several tens of μm long and contain between 10^4 and 10^6 mature collagen molecules. (29) Fibrillogenesis is the key factor in connective tissue morphogenesis. (30)

The major fibrillar collagens are water-soluble at low pH, for example in dilute acetic acid. When the pH is adjusted to around neutral and the temperature raised to around physiological, fibril formation occurs spontaneously resulting in banded fibrils. Fibrils are stabilized by the formation of covalent cross-links. (31) Fibrils are stable over a wide pH range of 6,2 – 12. The periodic stagger is constant at 66,5 nm and relates to the maximum interaction between oppositely charged side chains and large hydrophobic amino acids of adjacent triple helices. (32) (23)

Assembly proceeds by a nucleation and growth mechanism, during the lag phase, small numbers of collagen molecules associate to form metastable nuclei, upon which further molecules aggregate during the growth phase. The final step in the biosynthesis of collagen is the introduction of covalent cross-links to stabilize the different forms of supramolecular assembly. (24)

Collagen concentration is one of the most important factors affecting self-assembly, the lag phase is shortened as collagen concentration is increased. (31) (30) It has been suggested that during the lag phase, triple helices form small multimeric intermediates that later aggregate into ordered structures. Fibril growth

would then proceed by further addition of multimeric intermediates, the final size being governed by the number of collagen molecules available in solution. (30)

The development of mechanical properties during collagen gelation has currently been studied by rheology, as demonstrated by Yang and Kaufman (2009). (31) (32) The development of the gel viscoelasticity was monitored in time via oscillatory rheology, and the development of the collagen network was found to be consistent with the percolation theory of branched networks. To monitor mechanical properties during gelation, time-sweep rheology studies were performed, yielding new information on the structures that give rise to the mechanical properties of collagen gels during gelation as a function of collagen concentration and gelation temperature. (26)

2.4 BIOMINERALIZATION

One of the defining features of the rigid biological systems that comprise a significant fraction of the structural biological materials is the existence of two components: a mineral and organic component. The intercalation of these components occurs at the nano, micro, or mesoscale and often takes place at a more than one-dimensional scale. The mineral component provides strength, whereas the organic component contributes to the ductility. This combination of strength and ductility leads to high energy absorption prior to failure. (26)

2.5 COLLAGEN/HAP NANOCOMPOSITES

The mechanisms of interaction of collagen and hydroxyapatite are of scientific and practical interest, but are still not established clearly. Based on the results of experimental NMR investigations of Aminova et al. (2013) of collagen and water suspensions, it was shown that hydroxyapatite can form intermolecular complexes with collagen fragments by the interaction of calcium ions with a proline group, forming weak intermolecular bonds.

In coll/HAP composites, the most important interactions involved are electrostatic interaction between opposite charged components or hydrogen bonding. These interactions occur between nHAP particles, between different collagen hierarchical structures and also between the organic and inorganic phases.

Hydrogen bonding occurs inside the collagen molecule itself, between collagen molecules, fibrils and fibres; also in hydroxyapatite and between collagen and hydroxyapatite. Electrostatic interaction takes place especially between Ca^{2+} cations (from HAP) and carboxylate groups (from collagen) as well as between hydroxyapatite grains (especially between Ca^{2+} and the phosphate anions), inside collagen molecules and between collagen fibrils and fibers. (27)

2.6 HIERARCHICAL COLLAGEN-BASED TISSUES: BONE

Bone is a structural material that comprises the bulk of the vertebrate skeleton, its hierarchical structure has been described in a number of reviews. (28) (29) (30) Bone (or better: the ECM of bone) can be interpreted as a highly organized composite material. It is composed of assemblies of tropocollagen molecules and nanosized hydroxyapatite crystals, forming an extremely tough yet lightweight material. (28) (31) (29) Several different types of bone are known which differ concerning their hierarchical organization, but all types consist of a nanocomposite made of collagen type I and a mineral phase, hydroxyapatite (HAP) at the nanometer scale. (23) The main roles of bone are: to provide the mechanical support for the body, to protect the vital inner organs and also act as a mineral reservoir for Ca^{2+} and PO_4^{3-} . (27) (32)

The volume fraction distribution between the organic and mineral phase is approx. 60/40, making bone unquestionably a complex hierarchically structured biological composite. (1) (6) (8)

2.7 HYDROGEL VISCOELASTICITY

Hydrogels have gained great attention in the last decades, mainly due to their biomedical applications. Hydrogels are three-dimensional, hydrophilic polymeric networks capable of retaining large amounts of water or biological fluids, characterized by a soft and rubbery consistence, thus bearing similarity to living tissues. Because of their hydrophilicity and other unique properties such as biocompatibility and biodegradability, hydrogels can be exploited as scaffolds for tissue engineering (33) (34), carriers for drug delivery (35) and other biomedical applications. Hydrogels may be chemically stable or “reversible” (physical gels) stabilized by molecular entanglements and/or secondary forces including ionic, H-bonding or hydrophobic interactions. (36) (37)

Most hydrogels suffer from a lack of mechanical strength, as a result, few hydrogels are used to bear significant mechanical load in current applications. (38) (39) (40) The poor mechanical properties of hydrogels originate from their low resistance to crack propagation due to the lack of an efficient energy dissipation mechanism in the gel network (41) (42) To obtain hydrogels with a high degree of toughness, a number of techniques have been proposed such as topological gels (43), nanocomposite hydrogels (44), and double network (DN) hydrogels (45).

3 GOALS OF THE THESIS

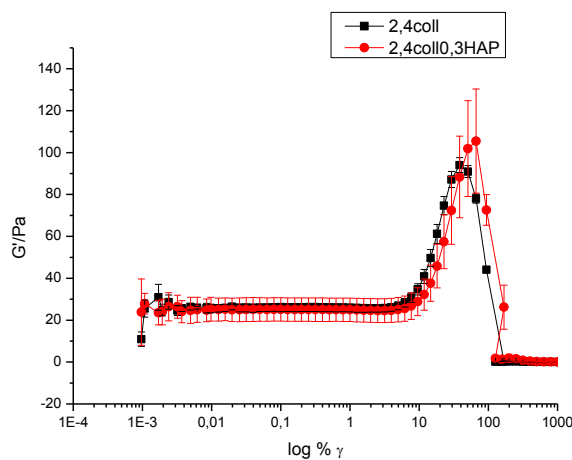
The primary aim of this Thesis is to investigate the mechanisms and kinetics of the self-assembly of pure collagen I and the effects of hydroxyapatite nanoparticles on collagen morphogenesis. The structural variables investigated will be collagen I concentration and nanohydroxyapatite content. The solutions and hydrogels will be investigated for mechanical and rheological properties under varying external conditions such as amplitude, time and mode of excitations. Still another goal of

the Thesis is to identify structural variables affecting the biomechanics of freeze-dried porous scaffolds made from these solutions and intended for bone and cartilage tissue engineering. Also the supramolecular structure of the collagen I/HAP nanocomposites will be studied, and the possible interaction modes of collagen-nanohydroxyapatite composites will be discussed. The effect of nanocomposite composition on the viscoelastic and rheological properties will be determined and an attempt to mathematically model the dependence of these properties on composition will be made. The emerging results will be discussed with possible motivation for future applications in tissue engineering and regenerative medicine.

4 RESULTS, DISCUSSION

4.1 DETERMINING THE LINEAR VISCOELASTIC INTERVAL

The storage and loss moduli G' and G'' , resp., were measured employing the 2° cone-plate geometry in dynamic oscillating mode using the AR G2 rheometer over a wide interval of shear strain amplitude (10^{-3} to 10^3). For neat collagen I solution 2,4 mg/ml as a model situation, the resulting dependence is depicted in Fig. 4.1.:



(a)

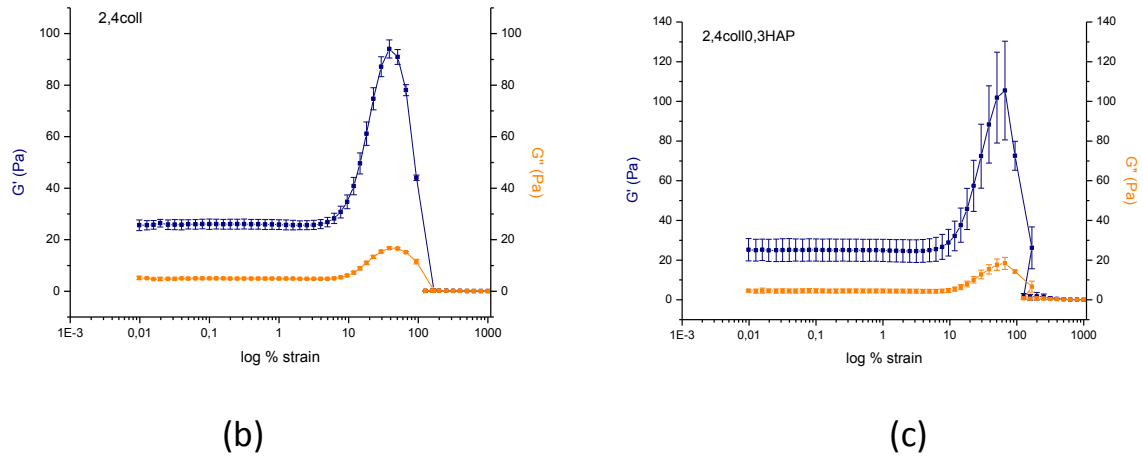


Fig.4.1. (a) The dependence of storage modulus G' on amplitude of shear strain γ for neat collagen solution (2,4coll) and collagen with added nHAP (2,4coll0,3HAP), presenting a linear viscoelasticity regime followed by strain stiffening and a breakdown of the self-assembled structure accompanied by a loss of the mechanical properties for shear strain amplitude between above 50%. The elastic modulus is zero for strains exceeding 100%. (b) G' and G'' for the neat 2,4coll, (c) G' and G'' for the 2,4coll,0.3HAP.

At low strains, $0,001\% \leq \gamma \leq 1\%$, the G' was relatively stable and constant (independent of shear strain amplitude) suggesting no structural transformation in the process. Above $\gamma \approx 10\%$, the G' increased significantly followed by a decrease to $G' \approx 0$ for $\gamma \geq 100\%$. This is a typical LAOS (large amplitude oscillatory shear) response of an associating system reflecting increasing rigidity of the existing 3D supramolecular structure followed by a collapse of the network due to mechanical disintegration. Since this behavior occurred for both neat collagen and coll/HAP nanocomposites, one can conclude that for the given composition, the response is fully related to the supramolecular structure of collagen. The maximum G' was slightly reduced by adding HAP as well as shifted towards lower shear strain amplitude. This may suggest that in the particular composition, HAP disrupts formation of the collagen supramolecular assembly as a result of partial depletion of the amine termini available for assembly due to interactions with HAP hydroxyls, as already shown in our published paper (57).

The fact that for both neat collagen and collagen/HAP nanocomposites the G'' is always lower than G' leads to a conclusion that the viscoelastic behavior of the systems investigated is controlled by the elasticity of the network with only a minor contribution from the viscous response. Collagen gels demonstrate elasticity derived predominantly from forming a hybrid cross-link network by crosslinking telopeptides and also from weak inter- and intra-molecular interactions. This means that the character of the viscoelastic response of the systems investigated resembles that of the bone matrix.

All the collagen solutions investigated exhibit a shear stiffening with increasing strain, characterized by a distinct peak formation, followed by a destruction of the formed structure and the collapse of the storage modulus towards zero. The extent of this strain stiffening (increase of G') was determined by subtracting the baseline value at 1% strain from the peak height. The experimental data fit (the full lines connecting the individual points) for moduli in both pure and nHAP modified collagen solutions) was best with an exponential function.

The nHAP addition did not affect the observed collagen strain-stiffening over a broad range of concentrations. However, the increase of collagen concentration in coll/HAP nanocomposite above 50 vol.% led to the exponential increase of $\Delta G'$ and $\Delta G''$ shown in Fig. 4.2. HAP nanoparticles strongly affect the ordering and relaxation dynamics of the surrounding collagen chains on the segment scale level, producing extensive changes of mechanical and physical properties on a much larger macro scale. It was found that for random NP packing, a significant portion of interparticle distances is shorter than the chain length necessary to form entanglements. Thus, the random particle packing is essential for enhancing chain incremental stiffness due to strong chain confinement *via* interaction with filler surfaces at much smaller filler content than predicted using uniform particle

spacing. We suggest that this is also the mechanism causing the substantial stiffening observed in our model systems.

Adsorption of chains onto nanoparticle surface leads to the creation of surface-chain loops and interparticle bridges. These chain segments can be relatively short and their conformation statistics deviates from the Gaussian behavior significantly. Under a given time scale of measurement, the average time of segment sorption/desorption event is long enough so that the non-Gaussian chains behave mechanically in a way similar to a covalent network. Sternstein's theory considers only changes of conformation entropy upon chain loading. As the chain extension approaches its limit, corresponding to r/Nb , the conformation entropy of a chain segment drops and the chain retractive force increases very rapidly. The retractive force can be then expressed as:

$$f = \frac{k_B T}{b} L^*(r/Nb), \quad (4.1)$$

where k_B is the Boltzmann constant, T is temperature and L^* is the inverse Langevin function, r is the chain end-to-end separation, N is number of monomer units and b is the monomer unit length. The elasticity of short chain segments has to take into account the bond angle, which is under given conditions almost undeformable. This leads to the correction that the full elongation of flexible chains corresponds to a maximum extension of $0.816Nb$ and not simply Nb . We used this model to analyze stiffening in coll/HAP nanocomposite substantially deviating from classical model predictions.

Our results indicate that a fully developed collagen gel was formed showing $G' > 10 G''$ and exhibiting plateau G' at low strain rates. Such an elastic response reflects the presence of an underlying network that is capable of storing elastic energy over long timescales. Three possible scenarios forming local constraints to molecular movement of collagen nanofibrils/triplehelices which may result in gelation are possible. They include attraction at junctions (a), spatial correlation

between adjacent molecules (b) and jamming at junctions (c) (59). The second scenario is relevant for the portion of collagen triplehelices participating in the formation of multiple nano and micro fibrils. The third scenario applies to growing rigid microfibrils the ends of which can jam into the bodies of adjacent fibrils. From the CLSM observations of large microfibril formation, it seems that the spatial correlation (mechanism (b)) is the dominant one in our case. Fibrils at different length scales are formed by a thermodynamically controlled transition from an angularly uncorrelated to a helical state. (60)

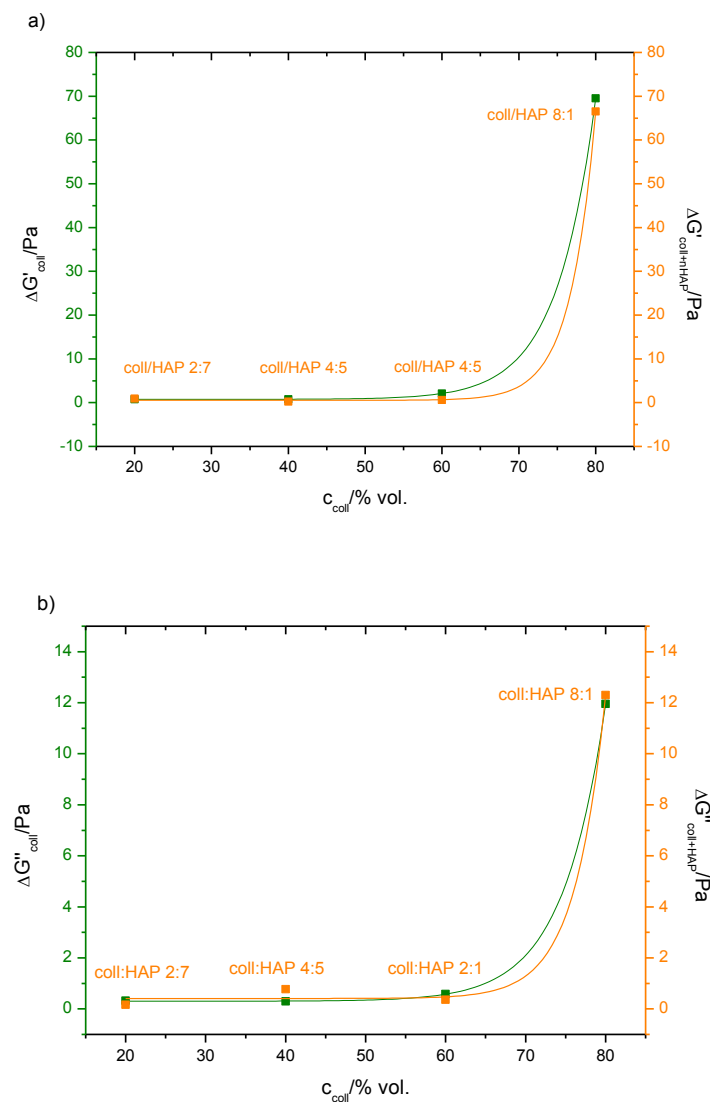


Fig.4.2. The composition dependence of the a) $\Delta G'$ and b) $\Delta G''$ (calculated from a baseline formed by the LVR) for both neat collagen and collagen with nHAP.

The shear strain amplitude at which the failure of the supramolecular structure had occurred was determined as the position of the $\Delta G'$ peak, beyond which mechanical stiffness decreases towards zero. For neat collagen, it was observed in the vicinity of the shear strain of 50 %. The effect of HAP addition resulted in a shift of this peak to greater strain amplitude, especially for 2,4coll0,3HAP, where the yield strain increased by 20%, thus a slight composition modification enhanced the mechanical properties of the resulting collagen-HAP nanocomposite, implicating an interaction at the molecular level that cannot be attributed to the individual components. In the less concentrated collagen solutions this effect was not statistically significant, see Fig. 4.3.

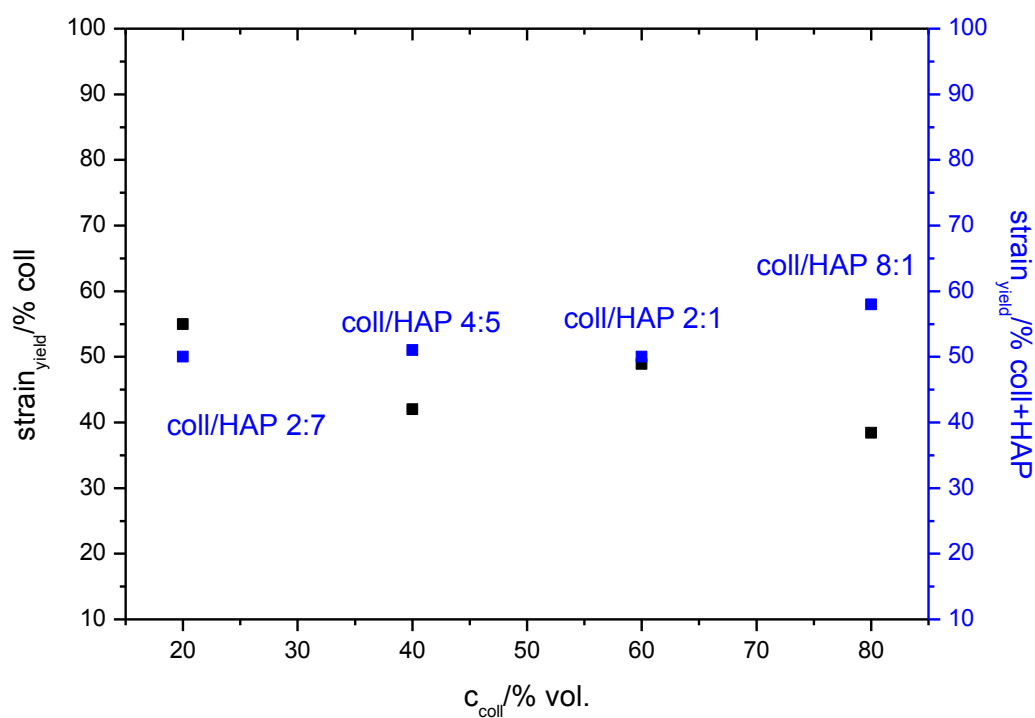


Fig. 4.3. The effect of nHAP addition on the yield strain.

4.2 REINFORCING MECHANISMS IN COLL/HAP NANOCOMPOSITE GELS

Any of the existing micromechanics models (61) predict the relative increase of the composite modulus over that of the neat matrix approximately only by a factor of 1.35 (35%). For comparison, the simple Guth-Gold model (61):

$$\frac{G_c}{G_m} = G_r = 1 + 2.5v_f + 14.1v_f^2, \quad (4.2.)$$

where v_f is the filler volume fraction, is plotted in Fig. 4.4b). Even the Mooney model (61) predicted an increase of the shear modulus, by adding $v_f = 0.15$, only 35% over the modulus of the neat matrix. Thus the observed several fold increase of storage modulus cannot be explained considering only the simple volume replacement reinforcement theory and molecular reinforcement mechanisms have to be taken into account.

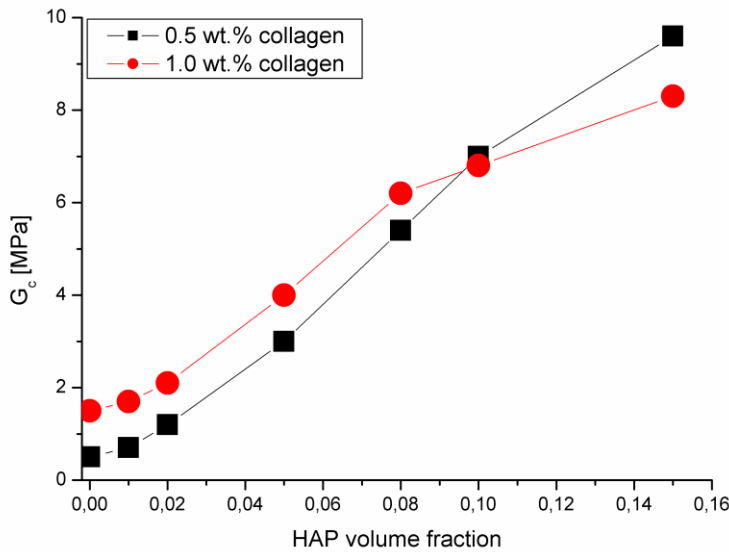


Fig. 4.4.(a) Concentration dependence of the shear modulus of the nanocomposites, G_c .

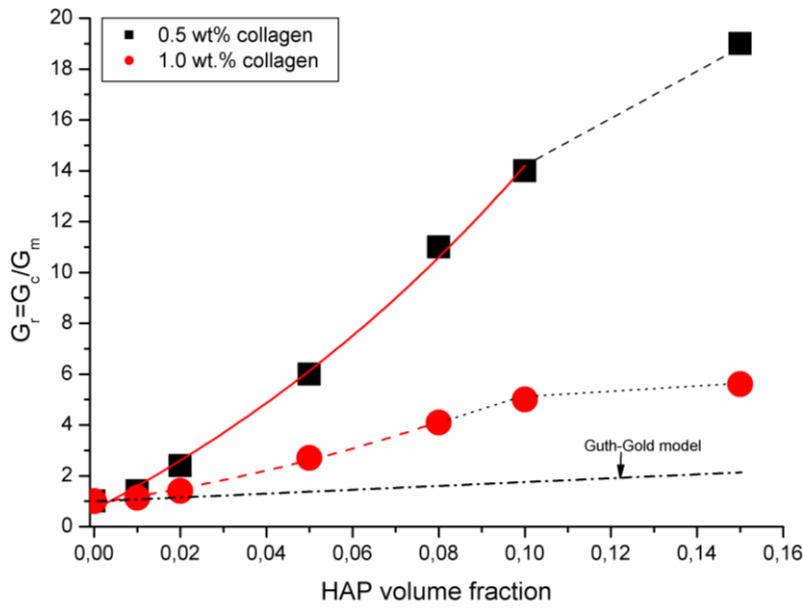


Figure 4.4.(b) Concentration dependence of the relative shear modulus of the nanocomposite, G_r . G_m is the modulus of a neat collagen matrix. Effect of the chain mobility on the reinforcing mechanism is evident from the difference between the 0.5 wt.% and 1.0 wt.% collagen. Comparison with simple volume replacement Guth-Gold (Eq. 4.2.) model is shown.

The interactions between collagen C-termini and OH- bonds on the HAP nanoparticles with dimensions on the same scale as the thickness of the tropocollagen triple helix have a tremendous effect on the retardation of their reptation dynamics (Fig. 4.7.). At the same time, the C-termini in the collagen phase become more depleted than the N-termini resulting in further reduction of collagen fibrillogenesis leading to a perturbation of the collagen network structure. In addition, the reduced mobility and chain confinement result in further disturbing the formation of collagen fibrils. As a result, the structure of the chemically cross-linked collagen network becomes more defective and dependent on the HAP content. On the other hand, the number of physical cross-links due to HAP-collagen interaction increases rapidly resulting in a much stiffer network (63) with rigidity strongly dependent on the strain level as described by the Mullins effect.

In order to obtain at least a qualitative comparison of experimentally observed behavior with theoretical prediction, the Co/HAP nanocomposite gel was considered a filled polymer network above its T_g . Since collagen resembles a worm like chain rather than a random Gaussian coil, Langevin rubber elasticity has been used. The Langevin rubber elasticity considers elasticity, which takes only changes of conformation entropy upon chain loading into account. As the chain extension approaches its limit, corresponding to $C(r/N_k l_k)$, the conformation entropy of a chain segment drops and the chain retractive force increases very rapidly; r is the worm like chain end-to-end distance, N_k is number of Kuhn segments and l_k is the segment length and C is the characteristic ratio. The retractive force of a worm like chain loaded in tension can be expressed as (64):

$$F(x) = \frac{kT}{L_p} \left[\frac{1}{4 \left(1 - \frac{x}{L_c} \right)^2} - \frac{1}{4} + \frac{x}{L_c} \right], \quad (4.3.)$$

where L_p is the persistence length, L_c is the contour length and x is the pulling distance. Substituting (κ_b/kT) for L_p yields:

$$F(x) = \frac{(kT)^2}{\kappa_b} \left[\frac{1}{4 \left(1 - \frac{x}{L_c} \right)^2} - \frac{1}{4} + \frac{x}{L_c} \right]. \quad (4.4.)$$

Considering Eq. 4.4., the retractive force of the collagen network can be expressed in the form:

$$f = \frac{(kT)^2}{2\kappa_b} L^{-1} \left(\frac{rkT}{2N_k \kappa_b} \right), \quad (4.5.)$$

where k is the Boltzmann constant, T is temperature and L^{-1} is the inverse Langevin function.

In order to demonstrate the effect of chain immobilization on the stiffening the Co/HAP nanocomposites, collagen network was modeled as a 3D tetrafunctional polymer network with affine cross-links. The model network was built to preserve the fundamental features corresponding to real collagen structure (Fig. 4.5.). At each node, three chains were considered flexible rubbery chains and the fourth one was marked as the collagen triple helix. During deformation of the neat network, the three flexible chains were deformed according to Langevin single chain elasticity:

$$\sigma = \frac{1}{3} E \sqrt{N_s} L^{-1} \left(\frac{\lambda_{chain}}{N_s} \right), \quad (4.6.)$$

where λ_{chain} is the draw ratio of chain, L^{-1} is the inverse Langevin function and N_s is a number of statistical segments. Length of the collagen triple helix chain was considered 280nm, and length of the flexible chain was calculated from the relation for a Kuhn chain model with 78 segments corresponding to 26 amino acids.

It has been shown that the presence of nanoparticles effectively alters the distribution of the length of chain segments towards the shorter segment lengths. These segments exhibit greater stiffness than the longer chain segments (Fig. 4.6.). For filler content of 1 vol%, segments with incremental stiffness higher than one effective entanglement strand represent about 5 % of polymer matrix. In a nanocomposite filled with 10 vol% of nanoparticles, such portion is already about 65% from the entire amount of polymer matrix. Thus, in nano-particle filled polymers, chain entanglements become a second-order interaction, while the “trapped entanglements” induced by non-penetrable filler nanoparticles become a first-order interaction. At the same time, randomly distributed solid HAP nanoparticles confine tropocollagen molecules significantly (Fig. 4.7.). Assuming random particle packing, the average interparticle distance reaches particle diameter for $v_f = 0.015$. (65)

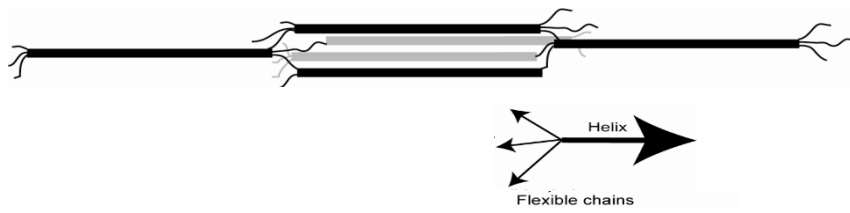


Figure 4.5. Schematic drawing of the simplified structure of the neat collagen network considered in the simple network model considering Langevin elasticity.

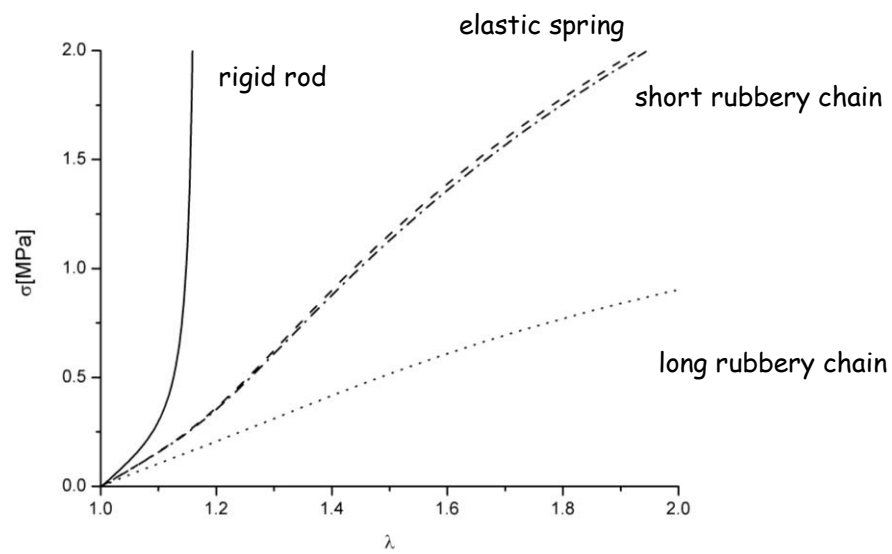


Fig. 4.6. Deformation response of a collagen network with varying the model used for deformation response of the collagen and assuming the Langevin rubber elasticity.

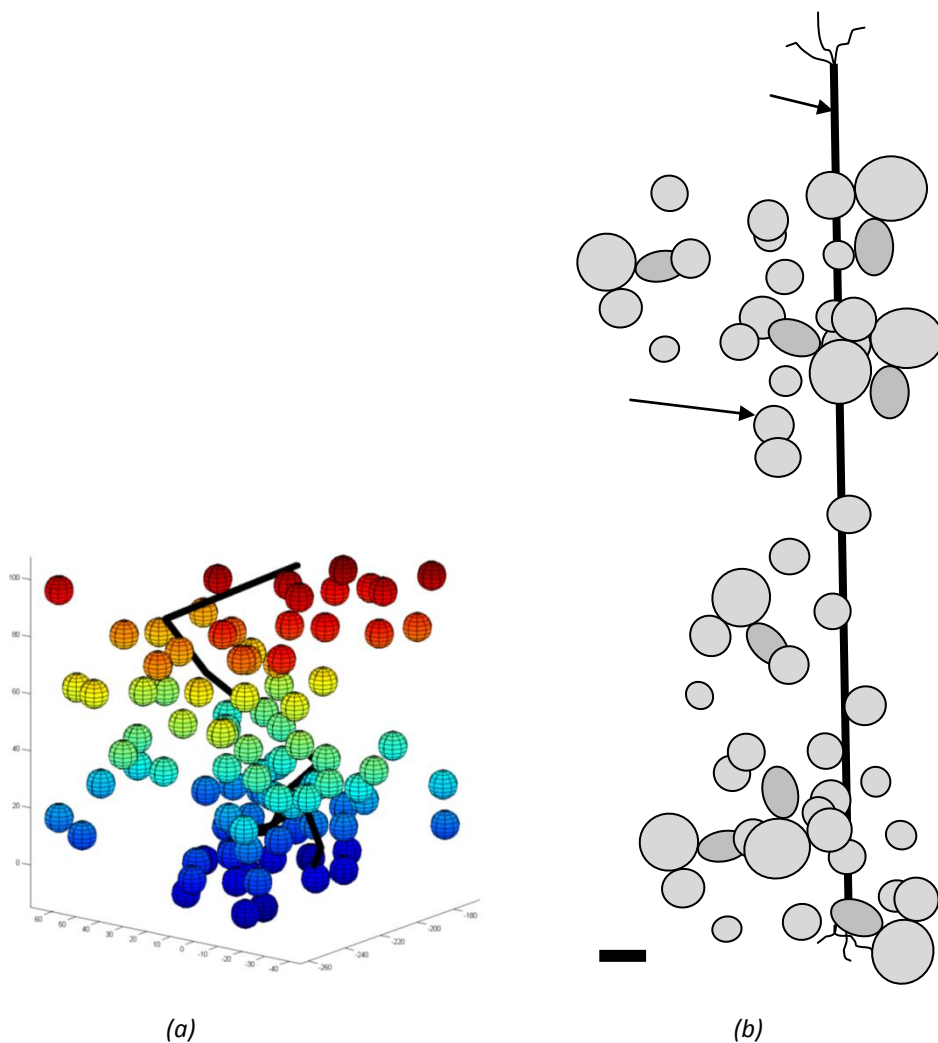


Fig. 4.7. a) Simulated random 3D distribution of monodisperse HAP nanoparticles and worm like collagen chain for 0.5 wt.% Co filled with 5 vol.% of HAP nanoparticles ($d=10$ nm). The distribution was generated using AGLOMER generator. Size of the simulated box is approximately $100\text{ nm} \times 100\text{ nm} \times 100\text{ nm}$. b) Schematic 2D drawing of the the ratio between volume occupied by collagen chain and HAP nanoparticles for 0.5 wt.% Co filled with 5 vol.% of HAP nanoparticles. For simplicity, collagen triple helix is shown in extended conformation. The area fractions occupied by collagen and HAP correspond with the composition of the Co(0.5)/HAP nanocomposite.

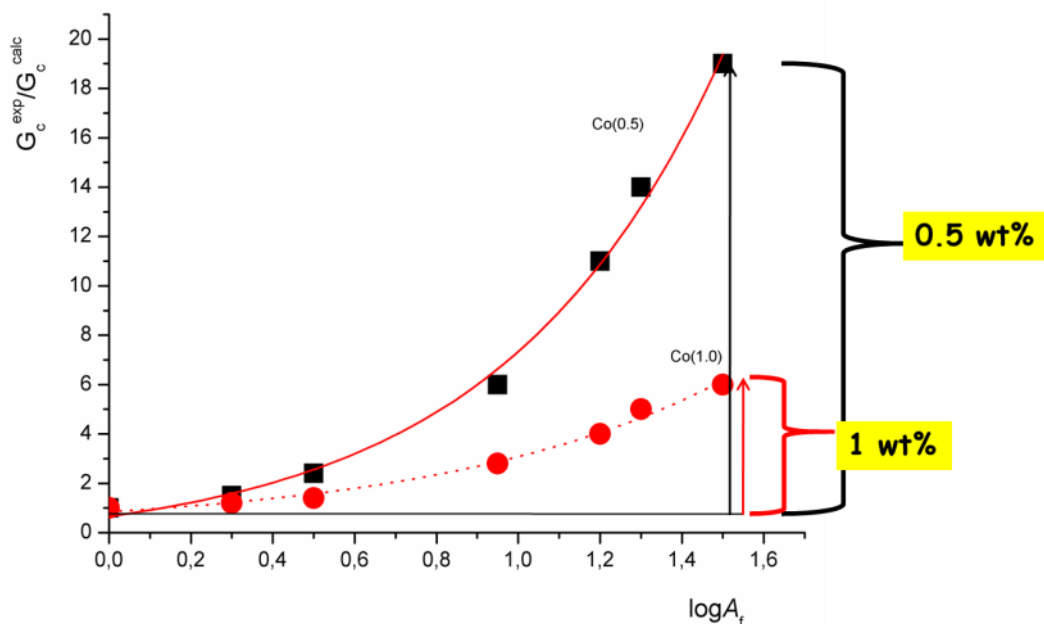


Fig. 4.8. Plot of the experimentally determined normalized shear storage modulus (symbols). Full and dotted lines represent contributions of molecular chain stiffening predicted using the model of Lin-Douglas-Horkay modified by Jancar et al (57).

The effect of HAP nanoparticle content incorporated into collagen on the storage moduli (G') of model nanocomposite gels containing was investigated. A simple chain reptation dynamics approach was used to describe the molecular reinforcing mechanism at the nano-scale and the controlling role of the area of contact between the matrix and the reinforcement. An "immobilized chain percolation network" with individual chains obeying Langevin rubber elasticity filled with randomly distributed HAP nanoparticles 20 nm in diameter was demonstrated to provide means for analyzing the meso-scale mechanical response of the Coll/HAP nanocomposite networks considering nano-scale structural information. In our analysis, the role of water in determining the G' has not been included and the behavior of the hydrogels was ascribed solely to the length scale independent viscoelasticity of the solid network. This approach seems a reasonable approximation for low solid content hydrogels formed by networks with strongly bound water enhancing the effective diameter of the network chains where the

contribution of the length scale dependent drag of water through the network does not contribute to the overall shear stress considerably.

4.3 KINETICS OF GELATION

The kinetics of collagen self-assembly was investigated employing dynamic oscillatory rheology by measuring the time evolution of viscoelastic moduli utilizing dynamic oscillatory time sweep, as described by Yang et al. (36). Collagen solutions of varying collagen and nHAP content were subjected to oscillatory shear under 1Hz frequency and 1% strain over a period of 90 minutes at physiological temperature of 37 °C. Solutions were neutralized and kept at 4 °C before measurement and the self-assembly was initiated at the beginning of the measurement by raising T to 37 °C. The mean value from three measurements is presented along with the standard deviation, which in all cases does not exceed 25%.

The collagen self-assembly proceeded in three phases as illustrated in Fig. 4.9. The initial phase corresponding to the breakdown of a weakly connected structure formed in the solution during the time between the sample preparation and measurement and manifesting itself by a decrease in the viscoelastic moduli. The minimum G' value is reached at $1.5 \cdot 10^3$ s indicating complete loss of elastic properties. The breakdown of a weakly associated structure is supported by the G'' being greater than G' during this stage, suggesting a rather viscous character of the response. In the second stage, the microfibril and fibril self-assembly occurs resulting in the change of the shear strain response from viscous liquid to viscoelastic gel manifested by G' being larger than G'' . At 2×10^3 s after reaching the minimum G' , a plateau G' is obtained signaling the completion of the self-assembly under the conditions of the experiment.

The evolution of the viscoelastic moduli in time for the neat and HAP modified 2,4coll, respectively, is shown in Fig. 4.10. (a) and (b), respectively. The obtained results are in agreement with those published in literature for neat collagen (31) (58). Collagen triplehelices assemble first in aggregates of 5-17 molecules (nuclei) followed by the assembly of these nuclei into microfibrils 30-300 nm in diameter with greatly variable length (36). Two or more of these microfibrils then assemble into bundles forming extended fibers that can branch and interconnect, thus forming a network. Formation of this structure is analogous to gelation observed in the course of thermoset cure. The development of collagen network was found to be consistent with the percolation theory of branched network formation (66). Interconnections between fibers are due to topological constraints formed by entanglements resulting in a complex physicochemical gel structure (35).

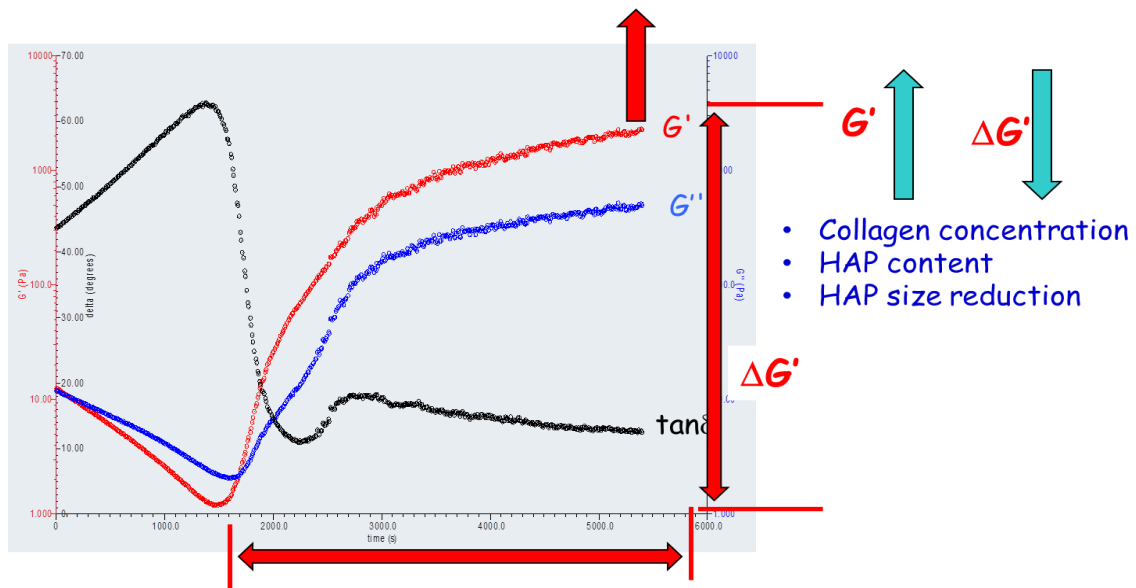


Fig. 4.9. Plot of the characteristic time dependence of the storage and loss shear modulus and $\tan\delta$ for collagen/HAP solutions measured at 37 °C and frequency of 1Hz showing the initial period, in which the structure formed between sample preparation and measurement is disassembled followed by the submicron fibril formation and reaching the network plateau modulus after approximately 2×10^3 s.

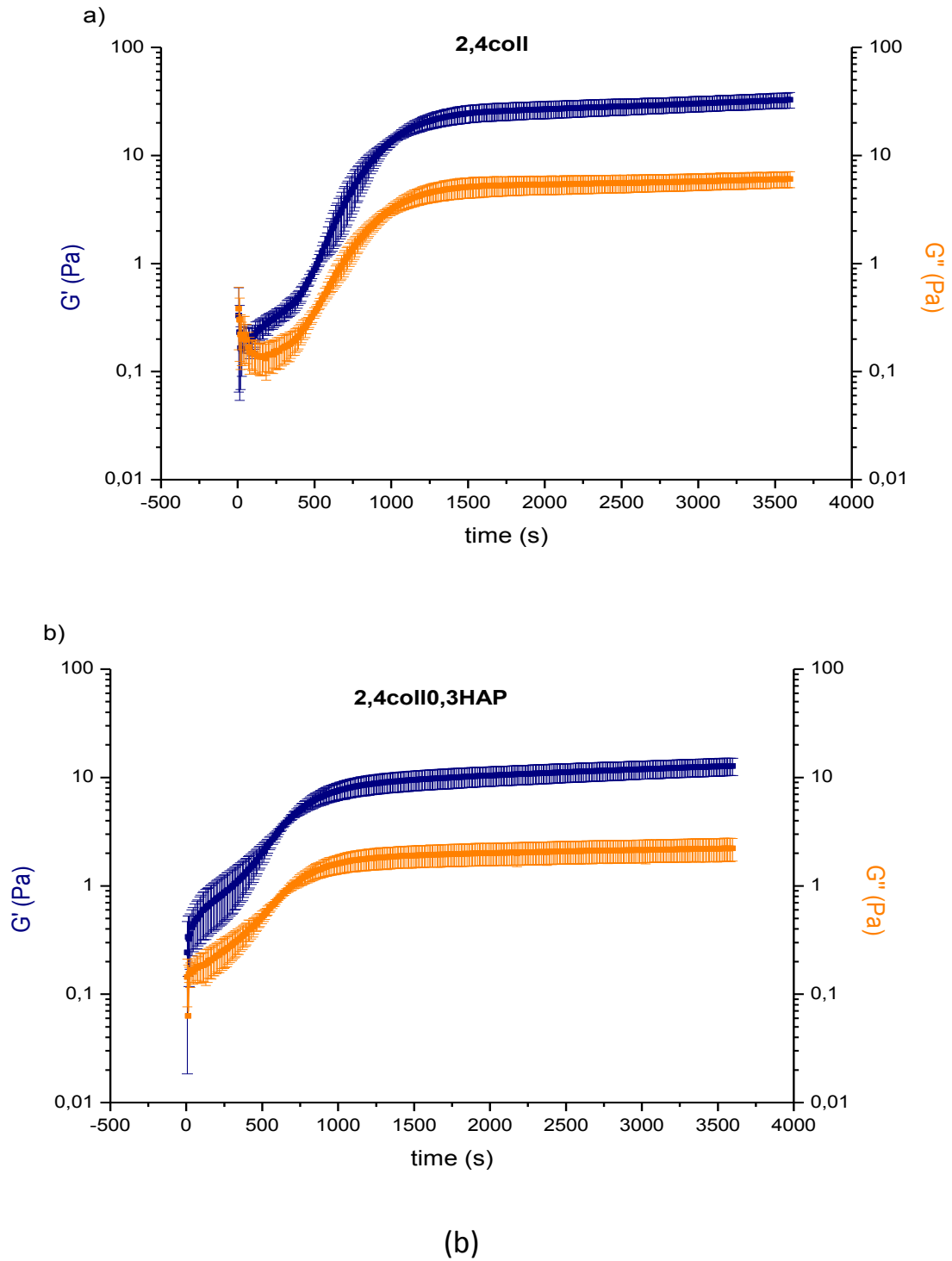


Fig. 4.10. a) The evolution of the viscoelastic moduli through time for neat collagen 2,4mg/ml. The self-assembled moduli plateaus are reached after $1,5 \cdot 10^3$ s .b) The evolution of the viscoelastic moduli through time for collagen 2,4mg/ml with 0,3mg/ml nHAP. The self-assembled moduli plateaus are reached after $1,0 \cdot 10^3$ s, suggesting the earlier onset of self-assembly compared to the neat solution facilitated by the presence of nHAP.

The addition of 0,3mg/ml nHAP did not change the character of the gelation kinetics significantly. Collagen and HAP concentrations control the plateau modulus obtained under given thermodynamic conditions. At this particular composition, however, the addition of nHAP results in a decrease of the viscoelastic plateau modulus, which contradicts the traditional wisdom of the volume replacement reinforcing mechanism. The plateau moduli are reached in $1,5 \times 10^3$ s for 2,4coll and at $1,0 \times 10^3$ s for 2,4coll0,3HAP. The earlier completion of collagen self-assembly can be explained by the bioactive nHAP facilitating acceleration of the self-assembly nuclei formation by weak interactions, but its low concentration results in a lower number of these nuclei. The time evolution of G' and G'' seems to follow the same functional form. This can be attributed to the fact that the process of collagen gelation by self-assembly and stiffening due to presence of rigid HAP are additive in nature.

The effect of nHAP addition on the viscoelastic moduli characterizing the ongoing self-assembly is shown in Fig. 4.11. for neat and HAP modified 2,4coll matrix. The resulting moduli of neat self-assembled collagen are higher compared to the nHAP modified system. At the same time, plateau modulus is achieved at shorter time for the HAP modified collagen. Considering the slope of the growth portion of the $G'(t)$ and $G''(t)$ as a measure of the rate of self-assembly, adding the HAP reduced the self-assembly rate significantly. This, along with the reduction of the absolute values of plateau G' and G'' , leads to a conclusion that HAP reduces the ability of collagen microfibrils to self assemble into larger fibers and hinders formation of the fibril network responsible for the gelation to occur. Our conclusions are in fair agreement with the rheological studies relating the size of the formed fibrils to the rheological behavior of collagen networks (58). Structurally, we propose that the amine termini of tropocollagen interact with the surface hydroxyls of HAP. This leads to a partial depletion of assembly controlling

amine termini from the collagen sol causing the observed drop in extent of gelation. This hypothesis is in agreement with the model of collagen fibrillogenesis proposed by Kadner et al. (67).

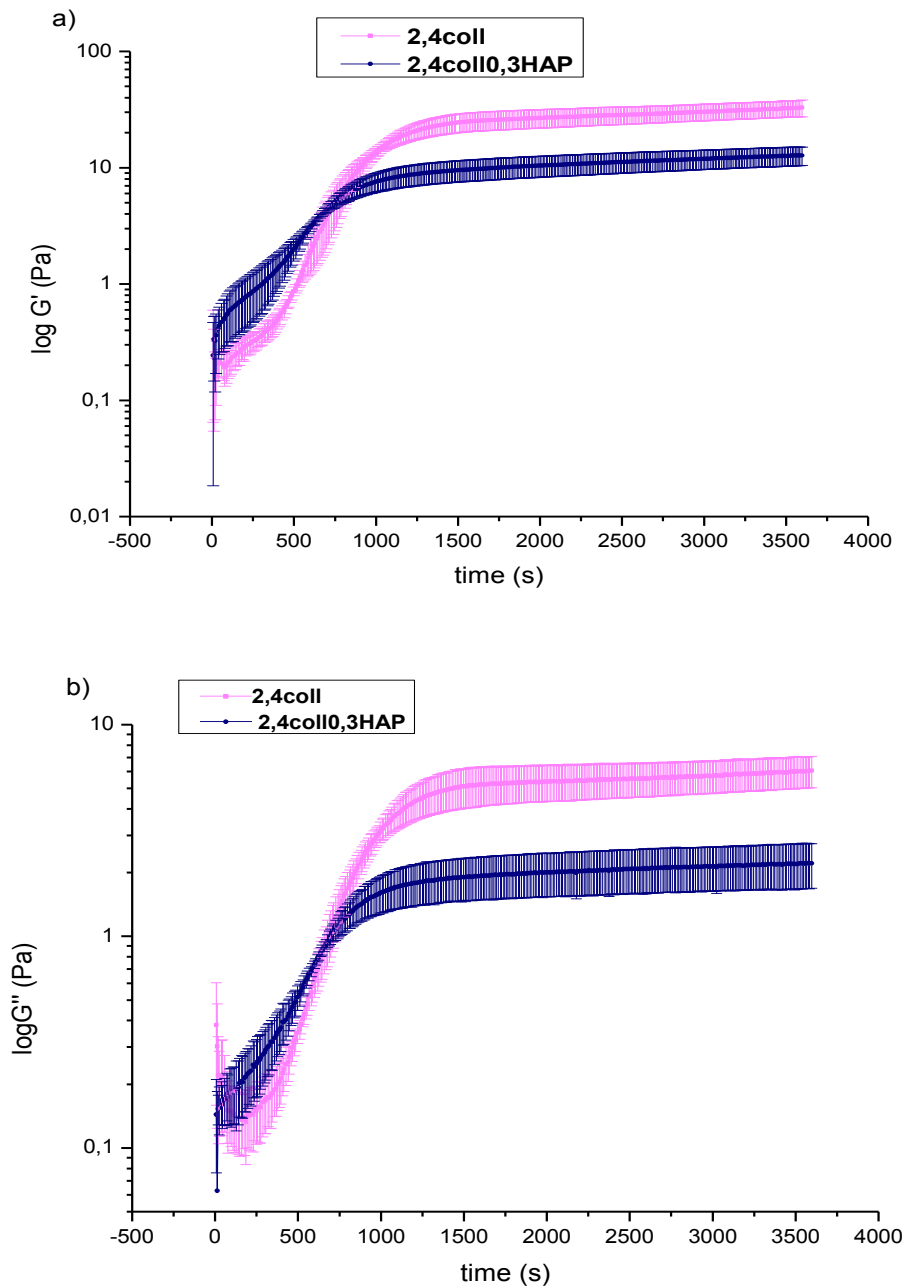


Fig. 4.11. a) The comparison of storage moduli time evolution for 2,4coll and its nHAP modified counterpart, 2,4coll0,3HAP. The onset of self-assembly takes place earlier in the nanocomposite, while the neat solution reaches a higher value of plateau storage modulus. b) A similar trend is observed for the loss moduli.

The addition of 0,3mg/ml nHAP did not change the character of the gelation kinetics significantly. Collagen and HAP concentrations control the plateau modulus obtained under given thermodynamic conditions. At this particular composition, however, the addition of nHAP results in a decrease of the viscoelastic plateau modulus, which contradicts the traditional wisdom of the volume replacement reinforcing mechanism. The plateau moduli are reached in $1,5 \times 10^3$ s for 2,4coll and at $1,0 \times 10^3$ s for 2,4coll0,3HAP. The earlier completion of collagen self-assembly can be explained by the bioactive nHAP facilitating acceleration of the self-assembly nuclei formation by weak interactions, but its low concentration results in a lower number of these nuclei. The time evolution of G' and G'' seems to follow the same functional form. This can be attributed to the fact that the process of collagen gelation by self-assembly and stiffening due to presence of rigid HAP are additive in nature. The results obtained in investigating the composition dependence of the kinetics of self-assembly are summarized in the Fig. 4.12.

For the neat collagen I, both the storage and loss moduli increased exponentially with increasing collagen concentration. The increase was steeper for the neat collagen systems compared to HAP modified collagen. However, when the coll/HAP ratio is lower than 1, a structure exhibiting large viscoelastic moduli (40-fold higher compared to the plateau values) is formed at the very beginning of the experiment. This structure is broken down during the first 500 s of the experiment leading to a significant drop in G' . For times longer than 500 s, the structure transformation proceeds toward the plateau moduli similarly to the nanocomposite networks with coll/HAP ratio greater than 1. In all cases, however, the plateau G' obtained for systems with coll/HAP ratio smaller than 1 is lower compared to gels with coll/HAP ratio >1 .

This phenomenon can be ascribed to the formation of large metastable HAP nanoparticle aggregates held together solely through weak short distance physical

HAP-HAP interactions. Thermodynamically, the controlling parameter is the decrease of the system enthalpy upon aggregation. In agreement with the Einstein–Stokes model of hydrodynamics of dispersion of particles in a liquid, systems with larger particles exhibit greater resistance to flow, thus, the G' and, especially, the G'' reach their maximum. As expected from the Einstein-Stokes model, greater effect is observed on the viscous portion of the response, e.g., on the G'' . The weak attractive HAP-HAP forces are acting over very short distance and, thus, they are unable to withstand the dynamic oscillatory shear forces throughout the entire measurement period. As a result, the formed HAP agglomerates are progressively disintegrated resulting in a reduction of their size causing significant drop of the hydrodynamic resistance of the system sol. At the same time, the entropy of the system grows due to improved dispersion of HAP nanoparticles. Then, tropocollagen self-assembly starts similarly to the neat systems, however, for the reasons mentioned above, collagen network formation is partially hindered by the HAP agglomerates resulting in smaller G' and G'' at the plateau.

The comparison of $G'(t)$ and $G''(t)$ dependences for various collagen solution compositions yields that the initial lag phase is shortened with increasing collagen concentration, which is consistent with the data and hypothesis established in literature (36). At the same time, adding the HAP nanoparticles extends the time needed to break down the structures formed between sample preparation and the measurement. It is also consistent with the hypothesis proposed previously, that between the sample preparation and measurement, reversible structures are formed that are disrupted and broken down by the dynamic oscillatory shear forces that they are subjected to when the measurement commences. Therefore, the initial test period must be considered more of a conditioning phase unifying the starting gel structure. Also, the phenomenon described above (the formation of a

temporary structure with high moduli caused by the abundance of nHAP) regarding samples with higher nHAP content, is observed.

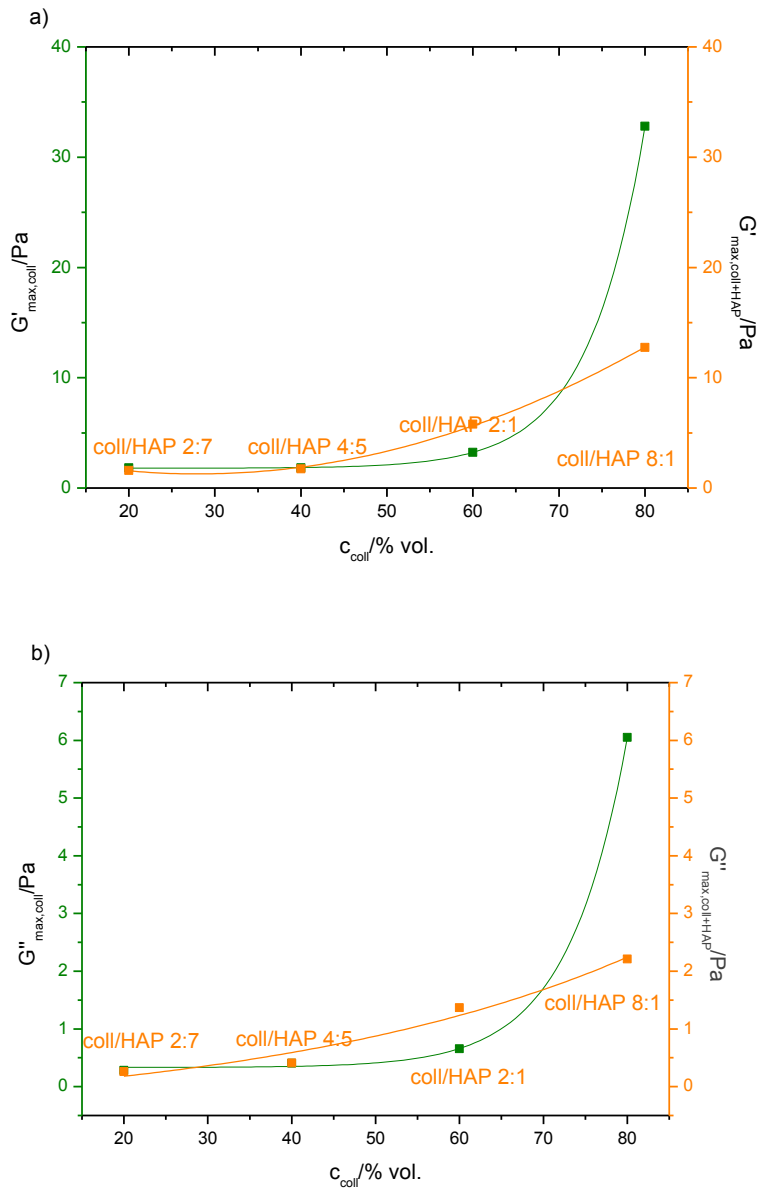


Fig. 4.12. a) The composition dependence of maximum self-assembled (plateau) storage moduli for neat collagen I solutions and collagen solutions containing nHAP. The storage modulus increases exponentially with increasing collagen concentration. b) The composition dependence of maximum loss moduli for pure collagen I.

The important results arising from these kinetic self-assembly experiments include that the viscoelastic plateau moduli increase exponentially with collagen concentration for neat collagen I solutions. This is in agreement with the model of worm like chain micelle self-assembly proposed in literature (60). For collagen I

with added nHAP, the resulting dependence is also exponential, but flatter. The crossover of the exponential fits is 70% collagen vol. concentration. Above this concentration, the collagen content dictates the self-assembly. During the first 500s, a peak in the elastic modulus and the formation of a viscoelastic network is observed, but during the following 500s, the structure breaks down and only a small plateau modulus appears after self-assembly. This suggests the formation of a reversible physical network structure with the increase of temperature at the start of measurement caused by an abundance of nHAP. This structure is however unstable and the weak interactions holding it together are broken within minutes. After 30 mins, the values of the elastic moduli approx. reach plateaus in all samples.

The dependence of mechanical properties on the system composition can be summarized as follows: the absolute value of the elastic modulus increases with the concentration of collagen, where more molecules are available for crosslink formation, also the more concentrated (less dilute) the solution, the more entangled the collagen chains become, also resulting in an increase in G' . The $\Delta G'$, however, decreases with the increase collagen concentration. This may be interpreted that in the first phase (which may be looked upon as a conditioning pre-shear step), only weak physical interactions are destroyed, however entanglement effects remain.

The nHAP addition results in a similar effect, although this cannot be attributed to entanglement, the sheer number of stiff nHAP particles contributes to an increase of G' during the entire experiment (the G' dependence is vertically shifted upwards and flatter, resulting in a $\Delta G'$ decrease). Also, the effect of the variation of nHAP particle size was studied, with decreasing nHAP particle size, an increase of G' was observed together with a decrease in $\Delta G'$. The smaller particles stiffen the structure more effectively, enabling closer packing of the collagen

molecules compared to the larger ones, which may in fact inhibit self-assembly by disabling the collagen molecules to move easily into close proximity necessary for higher-order structures to form.

4.4 THE DEPENDENCE OF VISCOSITY ON THE SHEAR RATE

The shear rate dependence of viscosity for neat collagen and nHAP modified collagen solutions was investigated using continuous shear flow measurements, unlike the experiments presented in the previous paragraph which were performed employing the oscillatory shear mode. Plots of viscosity as a function of the shear rate for systems with varying collagen concentration and/or HAP content, respectively, are shown in Figure 4.13. In Figure 4.14., the zero shear viscosity is plotted as a function of the collagen concentration and coll/HAP ratio.

All the systems investigated exhibited shear thinning behavior (see Fig. 4.13.), which is in agreement with the published data of Lai et al. (68). Addition of HAP did not change the character of their rheological behavior significantly regardless of the system composition. Adding nHAP caused reduction of the dependence of the high shear rate viscosity on the collagen content compared to the neat collagen gels (Fig. 4.13.). The shear rate viscosity data were extrapolated towards zero shear rate, as demonstrated by Tominaga et al. (69) and the extrapolated zero shear rate viscosities were plotted as a function of collagen concentration and nHAP addition (Fig. 4.14.). It was shown that the zero shear rate viscosity exhibits composition dependence similar to G' and, thus, similar models can be used for its structural interpretation.

There is a significant difference in the effect of collagen concentration on the zero shear viscosity between neat and HAP modified systems (Fig. 4.14.). While for neat collagen systems the dependence exhibits a high concentration viscosity limit (monotonous increasing asymptotic behavior), adding HAP results in a significant

drop in viscosity of at coll/HAP ratios below 1 followed by its steep increase. This is consistent with the systems' structure proposed in the previous paragraph. In the case of HAP modified collagen, the composition dependence of the zero shear viscosity seems to fit the Boltzmann S-shaped function with the inflection point near the 50 vol.% collagen. Such a behavior has been observed for systems exhibiting phase inversion. Since the HAP aggregates are disrupted by the shear flow, the zero shear viscosity remains almost constant or slightly decreases. In this region, the collagen self-assembly is effectively prohibited. Near the 50 vol% collagen, phase transition occurs resulting a collagen becoming the majority phase of the network capable of self-assemble to a small extent. As a result, the zero shear viscosity starts to increase with further decrease of the HAP content, eventually asymptotically approaching the neat collagen viscosity.

Also, the difference $\Delta\eta$ between the zero and maximum shear rate viscosity for neat and HAP modified collagen was plotted as a function of collagen content (see main document), where $\Delta\eta$ can be considered a measure of the extent of shear thinning. Again, this rheological behavior is consistent with the hypothesis of phase inversion put forward above.

These results may be interpreted that a small amount of added nHAP facilitates the formation of a reversible physical mineralized collagen network, where the intermolecular interactions maintain a more viscous character of the self-assembled gel. It seems that an over-abundance of nHAP may result in the formation of nHAP aggregates that do not promote self-assembly through sterical hindrance in the hypothetical gap regions. This can also explain the difference between properties of the coll/HAP gels prepared by mixing collagen with pre-synthesized nHAP particles and those prepared by in-situ precipitation of nHAP in the collagen gel as observed during formation of mineralized fibrils in healthy bone. Our results are, thus, strongly supportive of novel direction in preparing 3D

scaffolds for bone tissue engineering utilizing sol-gel nHAP or β -tri-calcium phosphate (β -TCP) precipitation at a certain stage of collagen fibril self-assembly.

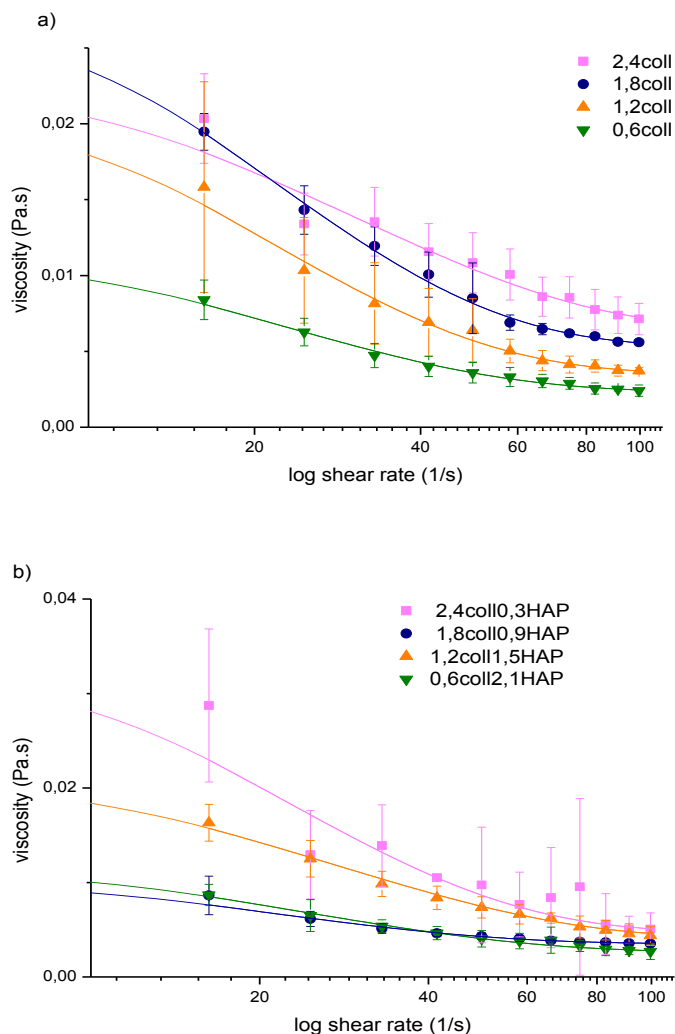


Fig 4.13. a) The dependence of viscosity on the shear rate for neat collagen solutions is similar for all measured concentrations with only a slight vertical shift downwards with decreasing concentration. The extrapolated data from the exponential fit are illustrated as full lines b) The dependence of viscosity on the shear rate for collagen solutions with the addition of nHAP is also a flat exponential, however the values converge towards a small interval with increasing shear rate. The extrapolated data from the exponential fit are illustrated as full lines.

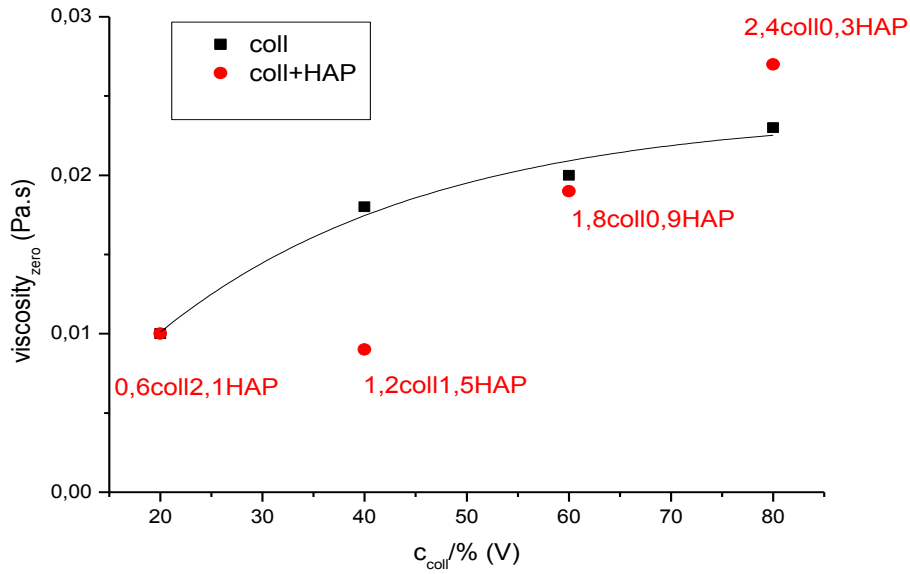


Fig. 4.14. The extrapolated zero shear rate viscosities for all measured collagen solution compositions. The addition of nHAP increases the viscosity only in 2,4coll0,3HAP. The fitted full line connecting the zero shear rate viscosity concentration dependence serves as a guide for the eye.

4.5 MORPHOLOGY OF FREEZE-DRIED COLLAGEN

An attempt was made to analyze formation of the microscale structure of self-assembled collagen and collagen/HAP nanocomposite microfibrils to ascertain the role of individual components in morphogenesis of the networks controlling the performance of their hydrogels.



Fig. 4.15. Photo of the 3D porous freeze-dried neat collagen network.

The freeze-dried porous collagen network was photographed at the macroscale (Fig. 4.15.) and at the micro-scale employing SEM (Figs. 4.16 and 4.17). The network was modified by adding HAP, or crosslinked by using carbodiimide chemistry prior to experiments and/or clinical trials using animal models to ensure the desired stability of the network.

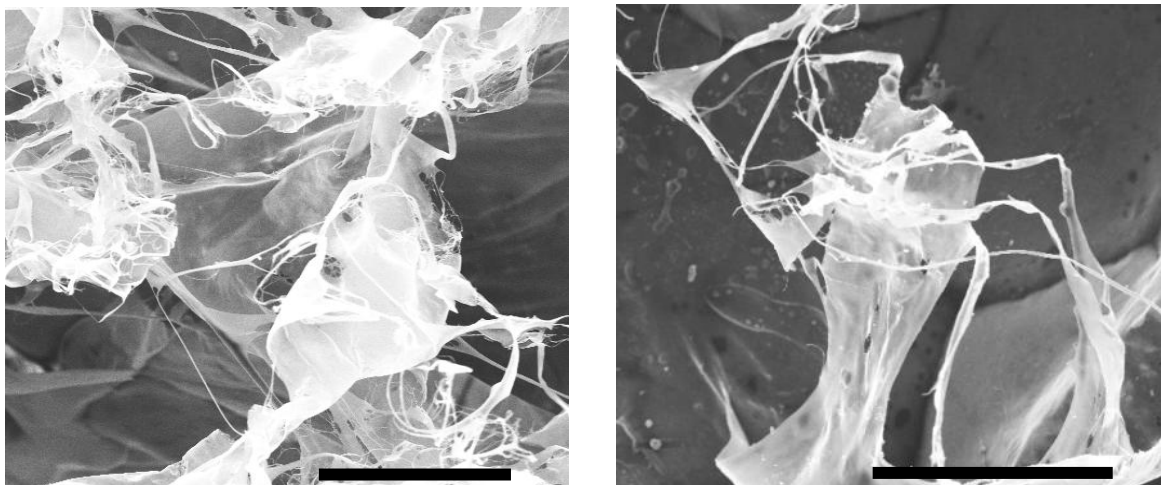


Fig. 4.16. SEM micrographs of freeze-dried porous uncrosslinked (left) and crosslinked (right) neat collagen network. Bar in the right lower corner represents 2 μ m.

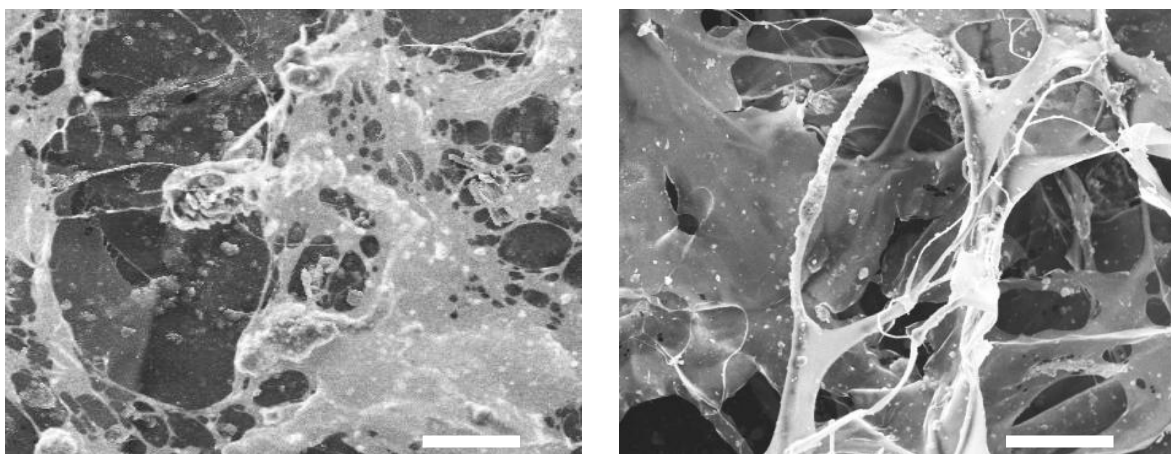


Figure 4.17. SEM micrographs of freeze-dried porous uncrosslinked (left) and crosslinked (right) collagen/HAP networks containing 20 wt.% hydroxyapatite nanoparticles. Bar in the right lower corner represents 20 μ m.

In all the cases investigated, morphology (supramolecular structure) of the 3D network consists of two basic structural elements. These are the elongated collagen fibrils and thin randomly oriented films forming walls between individual

pores originated from removal of water during freeze-drying. Adding HAP and/or cross-linking did not change the nature of the basic structural elements, however, affected the size of the fibrils and the compactness of the films. The cross-linking of neat collagen resulted in formation of larger diameter fibrils and thicker walls separating the pores in the freeze-dried self-assembled collagen network. Adding the nHAP resulted in two main structural differences compared to the neat collagen systems. First, addition of nHAP resulted in the disruption of some of the thin films separating the pores and a significant portion of nHAP deposited itself onto these films. Second, thin collagen fibrils formed in un-crosslinked collagen remained nHAP free most probably because of their small diameter providing insufficient attractive interaction for the nHAP particles of substantially greater diameter. Cross-linking greatly reduced the detrimental effect of nHAP on the pore wall structure and the larger fibrils were able to retain nHAP particles to a great extent, resulting in the formation of truly “mineralized” collagen fibrils.

4.6 USE OF FREEZE-DRIED COLLAGEN/HAP NETWORKS IN BONE TISSUE ENGINEERING

3D porous scaffolds were prepared by freeze-drying the coll/HAP nanocomposite hydrogels of different composition investigated in this work. These scaffolds were exploited in cell assays at the Institute of Experimental Medicine, CAS Prague, Faculty of Medicine, MU Brno and in clinical research of bone diseases and segmental defects at the Faculty of Veterinary Medicine, VFU Brno employing animal models. Results of this Thesis were utilized in determining the best coll/HAP network composition providing the desired balance of biomechanical properties, biological properties to host MSMs and surgical handling characteristics.

Neat collagen networks both native and cross-linked were used in treating defects in large joint cartilage in miniature pigs (Fig 4.18.) and the coll/HAP based

networks were used to prepare scaffolds for the regeneration of large bone segmental defects in rabbits (Fig. 4.20.). The MSCs attached to the scaffold (Fig. 4.19.) differentiated into osteocytes producing osteocalcine.

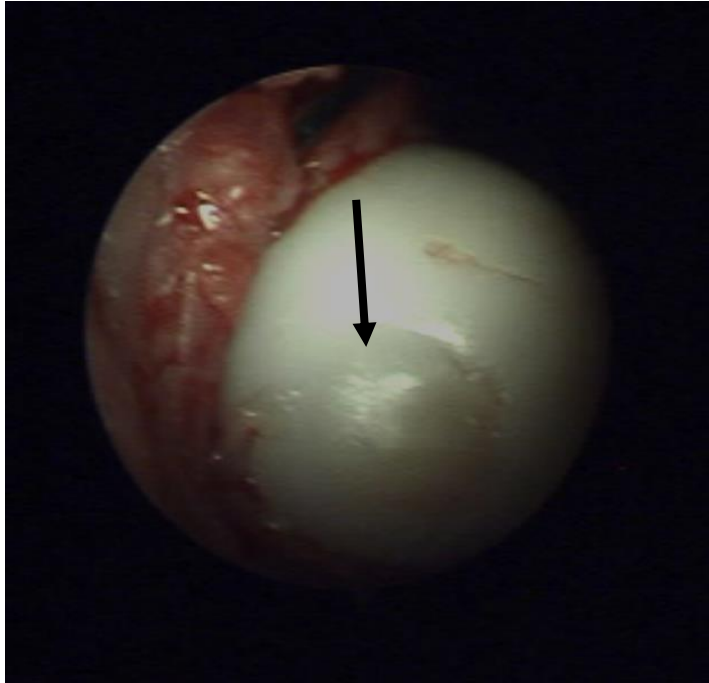
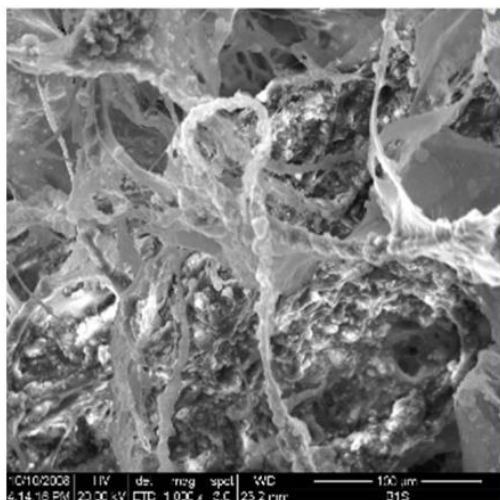


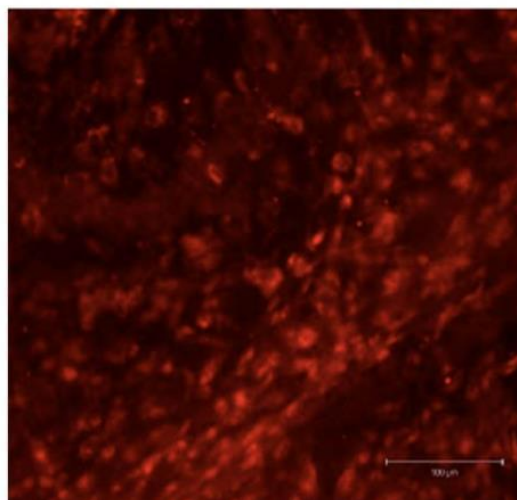
Fig. 4.18. Photograph of the newly formed hyaline cartilage in a condyle defect in miniature pig after 16 weeks healing period (arrow). The defect was treated with porous neat collagen scaffold seeded with 2×10^6 MSCs (courtesy of Professor A. Nečas, VFU Brno).

**Self-assembled Coll/HAP scaffold
with MSMs**



(a)

Osteocalcine after 28 days



(b)

Fig. 4.19. (a) SEM micrograph of the freeze-dried self assembled coll/HAP network scaffold seeded with MSCs clearly showing MSC attachment in the direction of collagen fibril orientation. (b) Ex vivo osteocyte secreted calcite after 28 days at 37 °C at pH 7. (right, courtesy of doc. A. Hampl, MU Brno).

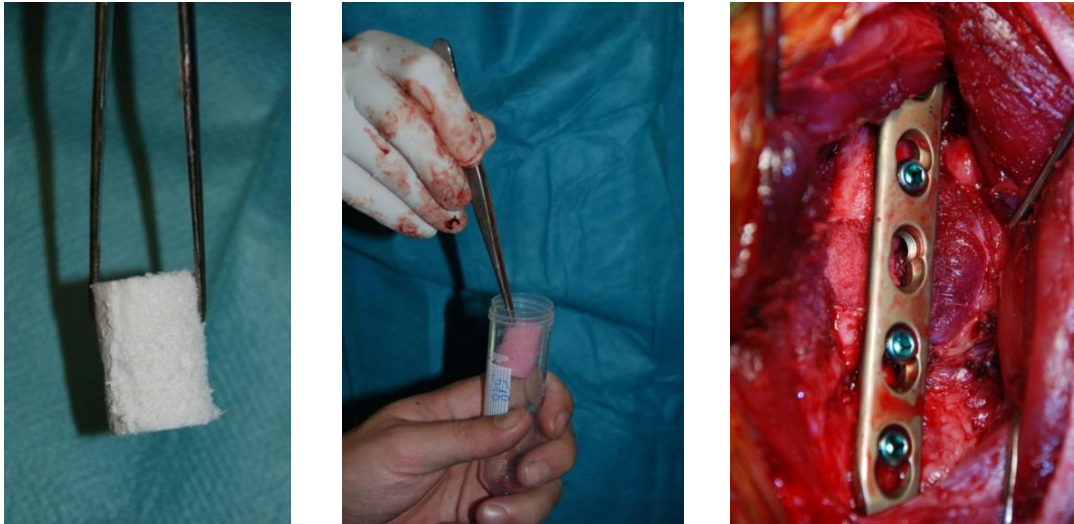


Fig. 4.20. Photograph of freeze-dried porous Coll/HAP scaffold (left) prior to MSC seeding. The Coll/HAP scaffold seeded with 2.6×10^6 MSCs prior to insertion during surgery to repair segmental defect in a rabbit (middle) and the scaffold after placement in tibia defect fixed with titanium plate (right) (courtesy of Professor A. Nečas, VFU Brno).

5 CONCLUSION

Tailored biomaterials with tunable functional properties are desirable for many applications ranging from drug delivery to regenerative medicine. To improve the ability to predict and “tailor” patient-specific properties and functions of biopolymer materials, multiple design parameters need to be considered, along with appropriate models.

The linear viscoelastic region (LVR) was determined by establishing a strain interval, where G' was independent of strain. The strain 1% was selected, which is in good agreement with other published data. The effect of matrix composition and HAP content on the shear storage modulus of the Co/HAP nanocomposites considered for manufacturing of porous scaffolds for bone tissue engineering was

investigated at 37 °C. The results showed that adding the HAP nanoparticles resulted in several fold increase in the storage modulus greatly above the predictions based on simple volume replacement micromechanics models. Hence, the proposed molecular reinforcement mechanisms are based on stiffening the worm like collagen chains *via* interactions with HAP nanoparticles resulting in retarded reptation in the vicinity of nanoparticles causing effective shortening of the rubbery network chains and percolation of HAP nanoparticle confined chains. This model provides reasonable framework for qualitative explanation of the observed concentration dependences of the storage modulus. Above $v_f=0.1$, the experimentally measured modulus negatively deviated from the predicted trend which has been attributed to the preferential interaction between the collagen C-termini and OH- groups of HAP resulting in their depletion. This caused deterioration of the network structure and, thus, reduction of its modulus. This fundamental finding can have implications in understanding the observed optimal HAP content in natural bone tissue.

The kinetics of self-assembly was studied using dynamic oscillatory shear time sweep rheology, following the time evolution of the viscoelastic moduli. The self-assembly initiated by a lag phase, followed by a growth phase accompanied by a steep increase in the storage modulus, suggesting the formation of an elastic collagen network. The nHAP did not enhance the value of this elastic modulus significantly, but facilitated the earlier onset of self-assembly through weak physical interactions. Also, in samples with nHAP/coll ratio higher than 1, a structure resulting from the presence of an abundance of nHAP with a high modulus was formed and broken down during the first 500 s.

All collagen solutions showed shear-thinning behavior fitted well by flat exponentials, which is in agreement with published research. The viscosity dependences were extrapolated towards zero shear rate in order to determine the

effect of composition. Also the decrease in viscosity (extent of shear thinning) was calculated and related to the nHAP content. The zero shear rate viscosity increased exponentially with increasing collagen concentration.

3D porous scaffolds were prepared by freeze-drying the coll/HAP nanocomposite hydrogels of different composition. Scaffolds with structure optimized based on results of this Thesis were utilized in treating defects in large joint cartilage in miniature pigs and for the regeneration of large bone segmental defects in rabbits.

6 REFERENCES

1. **Meyers, M.A., Chen, P., Lin, A.Y. and Seki, Y.** Biological materials: Structure and mechanical properties. *Prog.Mater.Sci.* 53, 2008, Vols. 1-206.
2. **Gronau, G., et al.** A review of combined experimental and computational procedures for assessing biopolymer structure-process-property relationships. *Biomaterials.* 33, 2012, Vols. 8240-8255.
3. **Gautieri, A., et al.** Viscoelastic properties of model segments of collagen molecules. *Matrix Biology.* 31, 2012, Vols. 141-149.
4. **Fratzl, P. and Weinkamer, R.** Nature's hierarchical materials. *Prog. Mater. Sci.* 52, 2007, Vols. 1263-1334.
5. **Espinosa, H.D., et al.** Merger of strcture and material in bone and nacre - Perspectives on de novo biomimetic materials. *Prog.Mater.Sci.* 54, 2009, Vols. 1059-1100.
6. **Gautieri, A., Vesentini, S., Redaelli, A., Buehler, M.J.** *Hierarchical structure and nanomechanics of collagen microfibrils from the atomistic scale up.* Milano : ACS Publications, NanoLetters, 2010.
7. **Buehler, M.J., Ackbarow, T.** Fracture mechanics of protein materials. *Materials Today.* September 2007, Vol. 10, 46-58.
8. **Yao, H.-B., et al.** Hierarchical assembly of micro/nano-building blocks: bio-inspired rigid structural functional materials. *Chem. Soc. Rev.* 40, 2011, Vols. 3764-3785.
9. **O'Brien, F.J.** *Materials Today.* 14, 2011, Vols. 88-95.
10. **Liu, X. and Ma, P.X.** *Annals of Biomedical Engineering.* 32, 2004, Vols. 477-486.

11. **Sionkowska, A. and Kozłowska, J.** Properties and modification of porous 3-D collagen/hydroxyapatite composites. *International Journal of Biological Macromolecules*. 52, 2013, Vols. 250-259.
12. **Bondar, B., Fuchs, S., Motta, A., Migliaresi, C., Kirkpatrick, C.J.** Functionality of endothelial cells on silk fibroin nets: Comparative study of micro- and nanometric fibre size. *Biomaterials*. 2008, Sv. 29, 561-572.
13. **Oreffo, R.O., Triffitt, J.T.** Future potentials for using osteogenic stem cells and biomaterials in orthopedics. *Bone*. 1999, Vol. 2, 5S-9S.
14. **Hollister, S.J., Lin, C.Y.** Computational design of tissue engineering scaffolds. *Comput. Methods Appl. Mech. Engrg.* 2007, Vol. 169, 2991-2998.
15. **Trojani, Ch., Boukhecha, F., Scimeca, J.-C., Vandenbos, F., Michiels, J.-F., Daculsi, G., Boileau, P., Weiss, P., Carle, G.F., Rochet, N.** Ectopic bone formation using an injectable biphasic calcium phosphate/Si-HPMC hydrogel composite loaded with undifferentiated bone marrow stromal cells. *Biomaterials*. 2006, Vol. 27, 3256-3264.
16. **Puppi, D, et al.** Polymeric materials for bone and cartilage repair. *Progress in Polymer Science*. 35, 2010, Vols. 403-440.
17. **Klapperich, C.M., Bertozzi, C.R.** Global gene expression of cells attached to a tissue engineering scaffold. *Biomaterials*. 2004, Vol. 25, 5631-5641.
18. **Badylak, S.F.** The extracellular matrix as a biologic scaffold material. *Biomaterials*. 2007, Vol. 28, 3587-3593.
19. **Wiedemann, A.L., Ahmad, M., Gutwald, R., Lauer, G., Hubner, U., Schmelzeisen, R.** How to optimize seeding and culturing of human osteoblast-like cells on various biomaterials. *Biomaterials*. 2003, Vol. 23, 3319-3328.
20. **Jansen, E.J.P, Sladek, R., Bahar, H., Yaffe, A., Gijbels, M.J., Kuijer, R., Bulstra, S., Guldemon, N.A., Binderman, I., Koole, L.H.** Hydrophobicity as a design criterion for polymer scaffolds in bone tissue engineering. *Biomaterials*. 2005, Vol. 26, 4423-4431.
21. **Shin, H.** Fabrication methods of an engineered microenvironment for analysis of cell-bioamterial interactions. *Biomaterials* . 2007, Vol. 28, 126-133.
22. **Buehler, M.J.** Nature designs tough collagen: Explaining the nanostructure of collagen fibrils. *PNAS*. 2006, Vol. 103, 12285-12290.
23. **Trus, B.L., Piez, K.A.** Molecular packing of collagen: three-dimensional analysis of electrostatic interactions. *J. Mol. Biol.* 1976, Vol. 108, 705-732.
24. **Gelinsky, M., Welzel, P.B., Simon, P., Bernhardt, A., König, U.** Porous three-dimensional scaffolds made of mineralised collagen: Preparation and properties of biomimetic nanocomposite material for tissue engineering of bone. *Chemical Engineering Journal*. 2008, Vol. 137, 84-96.
25. **Hulmes, D.J.S.** Collagen Diversity, Synthesis and Assembly. [book auth.] P. Fratzl. *Collagen Structure and Mechanics*. New York : Springer Science and Business Media, 2008.

26. **Whitesides, G.M. and Mathias, J.P.** Molecular self-assembly and nanochemistry. *Science*. 254, 1991, Vols. 1312-1319.
27. **Fertala, A., Sieron, A.L., Adachi, E. and Jimenez, S.A.** Collagen II containing a Cys substitution for arg-alpha1-519. *Biochemistry*. 40, 2001, Vols. 14422-14428.
28. **Steplewski, A., Hintze, V. and Fertala, A.** Molecular basis of organization in collagen fibrils. *J. Struct. Biol.* 157, 2007, Vols. 297-307.
29. **Kadler, K.E., Lightfoot, S.J. and Watson, R.B.** Biochemistry of the procollagen N-peptidase. *Methods Enzymol.* 1995.
30. **Parry, D.A. and Craig, A.S.** Growth and development of collagen fibrils in connective tissue. *Ultrastructure of the Connective Tissue Matrix*. 1984, Vols. 34-64.
31. **Gobeaux, F., Mosser, A., Anglo, A., Panine, P., Davidson, P., Giraud-Guille, M.M.** Fibrillogenesis in dense collagen solutions: A physicochemical study. *Journal of Molecular Biology*. 376, 2008, Vol. 1509.
32. **Fratzl, P.** Collagen - Structure and Mechanics. *Collagen: Structure and Mechanics, an Introduction*. New York : Springer Science+Business Media, 2008.
33. **Hulmes, D.J.S., Miller, A., Parry, D.A.D., Piez, K.A., Woodhead-Galloway, J.** Analysis of the primary structure of collagen for the origins of molecular packing. *J. Mol. Biol.* 1973, Vol. 79, 137.
34. **Yan, M., et al.** Effect of concentration, pH and ionic strength on the kinetic self-assembly of acid-soluble collagen from walleye pollock skin. *Food Hydrocolloids*. 29, 2012, Vols. 199-204.
35. **Forgacs, G., Newman, S.A., Hinner, B., Maier, C.W., Sackmann, E.** Assembly of collagen matrices as a phase transition revealed by structural and rheologic studies. *Biophys.J.* 2003, Vol. 84, 1272-1280.
36. **Yang, Y., Kaufman, L.J.** Rheology and confocal reflectance microscopy as probes of mechanical properties and structure during collagen and collagen/hyaluronan self-assembly. *Biophysical Journal*. 2009, Vol. 96, 1566-1585.
37. **Weiner, S. and Addadi, L.** At the cutting edge . *Science*. 298, 2002, Vols. 375-376.
38. **Ficai, A., et al.** Self-assembled collagen/hydroxyapatite composite materials. *Chemical Engineering Journal*. 160, 2010, Vols. 794-800.
39. **Weiner, S., Wagner, H.D.** *Annu. Rev. Mater. Sci.* 28, 1998, Vol. 271.
40. **Fratzl, P., et al.** *J. Mater. Chem.* 14, 2004, Vols. 2115-2123.
41. **Rho, J.Y., Kuhn-Spearing, L. and Zioupos, P.** Mechanical properties and the structure of bone. *Med. Eng. Phys.* 20, 1998, Vols. 90-102.
42. **Weiner, S., Traub, W., Wagner, H.D.** *J. Struct. Biol.* 126, 1999, Vol. 241.
43. **Bandyopadhyay-Ghosh, S.** Bone as a collagen-hydroxyapatite composite and its repair. *Trends in Biomaterials and Artificial Organs*. 22, 2008, Vols. 112-120.
44. **Drury, J.L. and Mooney, D.J.** Hydrogels for tissue engineering: scaffold design variables and applications. *Biomaterials*. 24, 2003, Vols. 4337-4351.

45. **Palumbo, F.S., et al.** Chemical hydrogels based on a hyaluronic acid-graft-elastin derivative as potential scaffolds for tissue engineering. *Mater.Sci.Eng.* 2013.
46. **Qiu, Y. a Park, K.** Environment-sensitive hydrogels for drug delivery. *Adv. Drug Delivery Rev.* 64, 2012, Sv. 49-60.
47. **Hoffman, A.S.** Hydrogels for biomedical applications. *Adv. Drug Deliv. Rev.* 43, 2002, Vols. 3-12.
48. **Peppas, N.A., et al.** Hydrogels in pharmaceutical formulations. *Eur. J. Pharm. Biopharm.* 50, 2000, Vols. 27-46.
49. **Gong, J.P., et al.** Double-network hydrogels with extremely high mechanical strength. *Adv.Mater.* 15, 2003, Vols. 1155-1158.
50. **Stevens, L., et al.** Ionic covalent entanglement hydrogels from gellan gum, carrageenan and an epoxy-amine. *Soft Matter.* 9, 2013, Vols. 3009-3012.
51. **Johnson, J.A., et al.** Some hydrogels having novel molecular structures. *Progress in Polymer Science.* 35, 2010, Vols. 332-337.
52. **Ahagon, A. and Gent, A.** Threshold fracture energies for elastomers. *Polym.Phys.Ed.* 13, 2003, Vols. 1903-1911.
53. **Brown, H.R.** A model of the fracture of double network hydrogels. *Macromolecules.* 40, 2007, Vols. 3815-3818.
54. **Okumura, Y. and Ito, K.** The polyrotaxane gel: a topological gel by figure-of-eight crosslinks. *Adv.Mater.* 13, 2001, Vols. 485-487.
55. **Sharifi, S., et al.** Biodegradable nanocomposite hydrogel structures with enhanced mechanical properties prepared by photo-crosslinking solutions of poly(trimethylene carbonate)-poly(ethylene-glycol)-poly(trimethylene carbonate) macromonomers and nanoclay particles. *Acta Biomaterialia.* 8, 2012, Vols. 4233-4243.
56. **Fei, R., et al.** Ultra-strong thermoresponsive double network hydrogels. *Soft Matter.* 9, 2013, Vols. 2912-2919.
57. **Jančář, J., Jančářová, E. and Žídek, J.** Combining reptation dynamics and percolation in modeling viscoelastic response of collagen based nanocomposites. *Journal of Computational and Theoretical Nanoscience.* 7, 2010, Vols. 1257-1264.
58. **Arevalo, R.C, Urbach, J.S. and Blair, D.L.** Size-dependent rheology of type I collagen networks. *Biophysical Journal.* 99, 2010, Vols. L65-L67.
59. **Raghavan, S.R. and Douglas, J.F.** *Soft Matter.* 8, 2012, Vol. 8539.
60. **Douglas, J.F.** *Langmuir.* 25, 2009, Vol. 8386.
61. **Buehler.** *Progress in Materials Science.* 53, 2008, Vols. 1101-1241.
62. **Fantner, G.E., et al.** *Biophysical J.* 90, 2006, Vols. 1411-1418.
63. **Sternstein, S.S. and Zhu, A.J.** *Macromolecules.* 35, 2002, Vols. 7262-7273.
64. **Zidek, J., Kucera, J. and Jancar, J.** *CMC.* 2010.
65. **Lin, D.C., Douglas, J.F. and Horkay, F.** Development of minimal models of the elastic properties of flexible and stiff polymer networks with permanent and thermo-reversible crosslinks. *Soft Matter.* 8, 2010, Vols. 3548-3561.

66. **Durand, D., et al.** *Europhys. Lett.* 3, 1987, Vol. 297.
67. **Kadner, K.E., Hill, A. and Canty-Laird, E.G.** *Current Opinion in Cell Biology.* 20, 2008, Vols. 495-501.
68. **Lai, G., Li, Y. and Li, G.** Effect of concentration and temperature on the rheological behavior of collagen solution. *International Journal of Biological Macromolecules* . 42, 2008, Vols. 285-291.
69. **Tominaga, T., et al.** The molecular origin of enhanced toughness in double-network hydrogels: A neutron scattering study. *Polymer.* 48, 2007, Vols. 7449-7454.
70. **Kadler, K.E., Hojima, Y. and Prockop, D.K.** Assembly of collagen fibrils de novo by cleavage of the type I pC-collagen with procollagen C-proteinase. *J.Biol.Chem.* 260, 1987, Vols. 15696-15701.

7 CURRICULUM VITAE

Jméno: Ema Jančářová
 Narozena: 9.2.1984 v Brně



Vzdělání

2003 – 2008 Masarykova univerzita v Brně, Přírodovědecká fakulta, obor Biofyzika Magisterské studium – obor Biofyzika zakončeno červeným diplomem.

Bakalářská práce: *Vliv povrchové energie zubních materiálů na depozici mikrobiálního plaku*

Diplomová práce: *Use of silver containing compounds as bacteriocides in dimethacrylate-based dental materials*

- 2009 – doposud Vysoké učení technické v Brně, Fakulta chemická, Ústav chemie materiálů, obor Chemie makromolekulárních materiálů
Dizertační práce: *Structure and properties of collagen/HAP nanocomposites*
- 2013 – doposud CEITEC – Středoevropský technologický institut, Brno, Research Group 2

Publikace

JANČÁŘ, J.; RECMAN, L.; JANČÁŘOVÁ, E. *Strain hardening in PMMA/ silica nanocomposites*. F: ESPCI Paris Tech, 2010. s. 36-37.

JANČÁŘ, J.; JANČÁŘOVÁ, E.; ŽÍDEK, J. Combining reptation dynamics and percolation in modeling viscoelastic response of collagen based nanocomposites. *Journal of Computational and Theoretical Nanoscience*, 2010, roč. 7, č. 7, s. 1257-1264. ISSN: 1546- 1955.

JANČÁŘ, J.; HOY, R.; LESSER, A.; JANČÁŘOVÁ, E.; ŽÍDEK, J. Effect of Particle Size, Temperature, and Deformation Rate on the Plastic Flow and Strain Hardening Response of PMMA Composites. *MACROMOLECULES*, 2013, roč. 46, č. 23, s. 9409-9426. ISSN: 0024- 9297.

Ostatní aktivity

Účast na projektu CHONDROS – příprava kolagenních scaffoldů pro tkáňové inženýrství – klinická studie ve spolupráci s VFU Brno

Pedagogická praxe – Praktikum Struktura a vlastnosti polymerů, FCH VUT v Brně,
Praktikum Struktura a vlastnosti kompozitů, FCH VUT v Brně